INFLUENCE OF EXTRINSIC FACTORS ON GUANIDINE HYDROCHLORIDE DENATURATION OF BACILLUS LICHENIFORMIS α-AMYLASE

SALANEE A/P KANDANDAPANI

FACULTY OF SCIENCE
UNIVERSITY OF MALAYA
KUALA LUMPUR

2016

INFLUENCE OF EXTRINSIC FACTORS ON GUANIDINE HYDROCHLORIDE DENATURATION OF BACILLUS LICHENIFORMIS α-AMYLASE

SALANEE A/P KANDANDAPANI

DISSERTATION SUBMITTED IN FULFILMENT OF THE REQUIREMENTS FOR THE DEGREE OF MASTER OF SCIENCE

INSTITUTE OF BIOLOGIGAL SCIENCES
FACULTY OF SCIENCE
UNIVERSITY OF MALAYA
KUALA LUMPUR

2016

UNIVERSITY OF MALAYA

ORIGINAL LITERARY WORK DECLARATION

Name of Candidate: Salanee Kandandapani   (I.C No: ███████)

Matric No: SGR 140039

Name of Degree: Master of Science

Title of Dissertation: "Influence of Extrinsic Factors on Guanidine Hydrochloride

Denaturation of *Bacillus licheniformis* α-Amylase"

Field of Study: Biochemistry

I do solemnly and sincerely declare that:

(1) I am the sole author/writer of this Work;
(2) This Work is original;
(3) Any use of any work in which copyright exists was done by way of fair dealing and for permitted purposes and any excerpt or extract from, or reference to or reproduction of any copyright work has been disclosed expressly and sufficiently and the title of the Work and its authorship have been acknowledged in this Work;
(4) I do not have any actual knowledge nor do I ought reasonably to know that the making of this work constitutes an infringement of any copyright work;
(5) I hereby assign all and every rights in the copyright to this Work to the University of Malaya ("UM"), who henceforth shall be owner of the copyright in this Work and that any reproduction or use in any form or by any means whatsoever is prohibited without the written consent of UM having been first had and obtained;
(6) I am fully aware that if in the course of making this Work I have infringed any copyright whether intentionally or otherwise, I may be subject to legal action or any other action as may be determined by UM.

        Candidate's Signature   Date:
        (Salanee a/p Kandandapani)

Subscribed and solemnly declared before

        Witness's Signature   Date:

Name:
Designation:

        Witness's Signature   Date:

Name:
Designation:

ABSTRACT

The influence of buffer composition on the conformational stability of native and calcium-depleted *Bacillus licheniformis* α-amylase (BLA) was investigated against guanidine hydrochloride (GdnHCl) denaturation using circular dichroism, fluorescence and UV-difference spectroscopy. Buffers used in these experiments were: 0.05 M sodium phosphate buffer, pH 7.5, 0.15 M Tris-HCl buffer, pH 7.5, 0.15 M HEPES buffer, pH 7.5 and 0.15 M MOPS buffer, pH 7.5. Differential effects of buffer composition on GdnHCl denaturation of BLA were evident from the magnitude of these spectral signals, which followed the order: sodium phosphate > Tris-HCl > HEPES > MOPS. These effects became more pronounced when calcium-depleted BLA was used in the incubation mixture as revealed by a lower relative mean residue ellipticity, lower relative fluorescence intensity, and higher change in emission maximum. Depletion of calcium from BLA suggested a decrease in the protein conformational stability. Gel chromatographic analyses of native, 3 M GdnHCl-denatured and 6 M GdnHCl-denatured BLAs were made in different runs on Sephacryl S-200 HR column (1.0×30 cm), equilibrated with these buffers. The results obtained clearly suggested formation of similar denatured states and aggregated forms of BLA in 3 M and 6 M GdnHCl in the presence of these buffers. However, quantitative differences in BLA aggregation were noticed in these buffers in the presence of 6 M GdnHCl. In view of the above, spectral results on BLA stability against GdnHCl obtained with different probes (MRE, fluorescence intensity and emission maximum) in different buffers should be treated with caution.

ABSTRAK

Pengaruh komposisi buffer terhadap penstabilan struktur asli dan ketiadaan-CaCl$_2$ *Bacillus licheniformis* α-amilase (BLA) yang dikaji dengan denaturasi menggunakan GdnHCl dengan 'circular dichroism' (CD), fluoresens dan 'ultraviolet' (UV) perbezaan spectroskopik. Buffer-buffer yang telah diselidik oleh kajian ini adalah: 0.05 M sodium phosphate buffer, pH 7.5, 0.15 M Tris-HCl buffer, pH 7.5, 0.15 M HEPES buffer, pH 7.5 and 0.15 M MOPS buffer, pH 7.5. Berbezaan kesan terhadap komposisi buffer dengan 'GdnHCl-denatured BLA' terbukti daripada magnitud isyarat spectrum, yang diikuti turutan sodium fosfat > Tris - HCl > HEPES > MOPS. Kesan-kesan ini menjadi lebih ketara apabila ketiadaan-CaCl$_2$ BLA dalam campuran pengeraman mendedahkan 'mean residue ellipticity' yang lebih rendah, relative intensiti fluoresens lebih rendah dan perubahan yang lebih tinggi dalam 'emission maksimum'. Ketiadaan-CaCl$_2$ BLA, mencadangkan kekurangkan penstabilan protein. Gel kromatografi analisis dengan sruktur asli, 3 M 'GdnHCl-denatured' dan '6 M GdnHCl-denatured BLAs' yang diperolehi dengan mengunakan Sephacryl S-200 HR column (1.0×30 cm), dengan buffer-buffer ini. Hasil kajian yang diperolehi, jelas mencadangan persamaan dalam penghasilan bentuk denaturasi dan agregat BLA dalam struktur asli, 3 M 'GdnHCl-denatured' dan 6 M 'GdnHCl-denatured' dengan kehadiran buffer-buffer ini. Bagaimanapun, kuantitatif perbezaan dalam BLA agregat telah diperhati mengunakan buffer-buffer ini dengan kehadiran 6 M GdnHCl. Oleh itu, keputusan spektrum yang menunjukkan kestabilan BLA patut disimpulkan dengan berhati-hati dengan kehadiran pengagregatan.

ACKNOWLEDGEMENTS

A special thought is devoted to my parents, Mr. Kandandapani Muthucanum and Mrs. Thanam Muniandy for a never-ending support. I am fortunate to have moral encouragement and inspiration from my husband, Mr. Tines Kumar and family, which endowed me the energy to complete this research.

<div align="center">

SALANEE KANDANDAPANI

June 2016

</div>

.

TABLE OF CONTENTS

LIST OF FIGURES

LIST OF TABLES

LIST OF SYMBOLS AND ABBREVIATIONS

BAA   *Bacillus amyloliquefaciens* α-amylase

BLA   *Bacillus licheniformis* α-amylase

BStA   *Bacillus stearothermophilus* α-amylase

BSUA   *Bacillus subtilitis* α-amylase

c   Concentration

$CaCl_2$ Calcium chloride

CD   Circular dichroism

cm   Centimeter

3-D   Three-dimensional

Da   Dalton

deg   Degree

$dmol^{-1}$ Per Decimole

ε   Extinction coefficient

EDTA   Ethylenediaminetetraacetic acid

GdnHCl   Guanidine hydrochloride

h   Hour

HEPES   4-(2-Hydroxyethyl)piperazine-1-ethanesulfonic acid sodium salt

i.e.	*id est* (that is)
l	Optical path length
M	Molar
min	Minute
mL	Milliliter
MOPS	3-(N-morpholino)propanesulfonic acid sodium salt
MRE	Mean residue ellipticity
MRE_{222nm}	Mean residue ellipticity at 222 nm
MRW	Mean residue weight
MW	Molecular weight
T_m	Melting temperature
Tris-HCl	Tris(hydroxymethyl)aminomethane-hydrochloride
Trp	Tryptophan
Try	Tyrosine
UV	Ultraviolet
V_e	Elution volume
V_0	Void volume
µM	Micromolar

INFLUENCE OF EXTRINSIC FACTORS ON GUANIDINE HYDROCHLORIDE DENATURATION OF
BACILLUS LICHENIFORMIS α-AMYLASE

INTRODUCTION

1. INTRODUCTION

α-Amylases are among the most important enzymes used in modern industry due to their application in the production of maltodextrin, alcohol, detergent, baking and textile industries (Pandey et al., 2000; Ammar et al., 2002; Bessler et al., 2003; Nagarajan et al., 2006). α-Amylases can be obtained from plants, animals and microorganisms. However, bacterial and fungal enzymes dominate the applications in the industrial processes (Souza and Magalhaes, 2010). *Bacillus licheniformis* α-amylase (BLA) has been the most popular enzyme in the present industry due to its remarkable thermostability (T_m ~103°C), (Declerck et al., 2002; Fitter and Haber-Pohlmeier, 2004) In fact, being a thermophilic enzyme from a mesophilic organism, BLA is even more thermostable than other α-amylases from thermophilic organisms, *e.g. Bacillus amyloquefaciens* α-amylase (BAA) and *Bacillus stearothermophilus* α-amylase (BStA) (Tomazic and Klibanov, 1988). Therefore, BLA has been the choice of many researchers to reveal the structure-fuction relationship of amylases (Tomazic and Klibanov, 1988; Machius et al., 1995; Khajeh et al., 2001, Nazmi et al., 2006). Although BLA shows similarity in the number of amino acid residues and molecular weight with other amylases, it possesses a much longer half-life ($T_{1/2}$ ~ 270 min) than other amylases (Table 1.1) under similar conditions (Tomazic and Klibanov, 1988). The presence of a few salt bridges in BLA, which are absent in BAA might be responsible for its higher thermostability (Tomazic and Klibanov, 1988; Machius et al., 1995). Furthermore, calcium ions have also been found to increase the thermal stability of BLA (Vihinen and Mantsala, 1989; Violet and Meunier, 1989; Feller et al., 1999). In view of the resistance towards chemical denaturation, shown by thermophilic proteins (Griffin et al., 2003), it would be of interest to study GdnHCl denaturation of BLA under different experimental conditions. Recently, a few papers have been published on GdnHCl denaturation of BLA, suggesting the importance of calcium and lysine residues

Table 1.1 Properties of several α-amylases from *Bacillus* species.

Property	*Bacillus licheniformis*	*Bacillus amyloliquefaciens*	*Bacillus stearothermophilus*
No. of residues	483 (Yuuki et al., 1985)	483 (Takkinen et al., 1983)	515 (Nakajima et al., 1985)
Molecular weight (Da)	58 000 (Damodara Rao et al., 2002)	54 778 (Takkinen et al., 1983)	78 000 (Inagaki et al., 1986)
Identity with BLA (%)	100 (Declerck et al., 2002)	81 (Declerck et al., 2002)	64 (Declerck et al., 2002)
*Half-life ($T_{1/2}$ min)[*]	270 (Declerck et al., 2002)	2 (Declerck et al., 2002)	50 (Declerck et al., 2002)
Melting temperature	101 (Fitter & HaberPohlmeir 2004)	86 (Fitter & Haber-Pohlmeir 2004)	-

*Half-life of these enzymes was determined at 90°C, pH 6.5 (Tomazic & Klibanov, 1988

towards its stability (Strucksberg et al., 2007; Tan et al., 2011). The role of other extrinsic factors in BLA stabilization remains to be explored.

Problem statement

In view of the above, several research questions arose in mind:

1) Does buffer composition affect the GdnHCl denaturation behavior of BLA?

2) Is the stabilizing effect of calcium on BLA similar in different buffers?

3) Does buffer composition affect GdnHCl-induced aggregation of BLA?

Objectives of the study

In order to address the above questions, the work presented in this dissertation was undertaken with the following objectives:

1) To study the effect of different buffer composition on GdnHCl denaturation of native BLA.

2) To study the effect of different buffer compositions on GdnHCl denaturation of calcium-depleted BLA.

3) To study GdnHCl-induced aggregation of native BLA in the presence of different buffers.

LITERATURE REVIEW

2. LITERATURE REVIEW

2.1 Background

Proteins preserve their native globular structures in order to display their biological functions. This conformational state of a protein, unique to itself, is formed as a result of folding involving different non-covalent interactions and disulfide bonds. Hydrophobic interactions and hydrogen bonds play an important role in stabilizing most proteins (Tanford, 1997; Machius et al., 2003; Ahmad et al., 2005; Pace et al., 2009). Under specific conditions *i.e*. pH, temperature, pressure and salinity, a protein has to maintain its native globular structure to prevent loss of biological activity (Imoto, 1973; Fagain and Kennedy, 1991; Fagain, 1995). An enzyme's biological activity in solution is built upon its three-dimensional conformation, which in turn is governed by its amino acid sequence (Anfinsen, 1973). About ~23 % of the total number of amino acid residues are distributed at the surface of the protein (Miller et al., 1987; Isom et al., 2010). Maintenance of the native structure of the protein is highly dependent on the environment (habitat) in which the organism thrives. Although thermophilic and mesophilic proteins are obtained from different sources, they are very similar in their native folded conformation (Arnold et al., 2001; Motono et al., 2001; Shiraki et al., 2004; Luke et al., 2007). Elucidation of the mechanism of thermostability of these proteins, has been made by various groups using techniques such as site-directed mutagenesis and chemical modification (Declerck et al., 1990; Declerck et al., 1995; Singh and Kayastha, 2014; Oliveira et al., 2015). Amylolytic α-amylase is a good example representing thermophilic protein, which can be obtained from both thermophilic and mesophilic organisms (Declerck et al., 2002; Fitter, 2005). It offers greater advantage as a source of enzyme for industrial use, which in most cases involves endothermic processes (Sterner and Liebl, 2001; Vieille and Zeikus, 2001).

Any structural alteration in the protein molecule may affect its function. Incorrect folding of a protein along with nonspecific interactions among various side chains may result in protein aggregation leading to the development of many protein folding diseases such as prion, Alzheimer and Parkinson's diseases (Zhang et al., 1995; Wood et al., 1996; Selkoe, 2004; Broadley and Hartl, 2009). Exposure of a protein to chemical denaturants during operational conditions of many industrial processes may lead to the loss of its function (Alonso and Dill, 1991; Pace et al., 2000; Iyer and Ananthanarayanan, 2008). Therefore, a detailed understanding about the mechanism of protein folding and protein stability involving the characterization of various intermediates and denatured states of a protein are essential (Ptitsyn et al., 1990; Ramos et al., 2004; Gianni et al., 2007; Sancho, 2013; Tsytlonok and Itzhaki, 2013). The most common chemical denaturants used for the protein denaturation studies are urea and guanidine hydrochloride (GdnHCl) (Tanford, 1968; Rizzolo and Tanford, 1978; Alonso and Dill, 1991; Dill and Shortle, 1991). These denaturants weaken both hydrophobic as well as polar interactions at higher concentrations (Dill and Shortle, 1991).

α-Amylases (α-1,4-glucan-4-glucanohydrolases, EC 3.2.1.1) are members of the endo-amylase family and catalyze the cleavage of α-D-(1,4) glycosidic linkages of starch (Machius et al., 1995; Pandey et al., 2000; Fitter, 2005). These enzymes are long established in industries involving starch processing, beverage, textile and detergent technologies (Asghari et al., 2004). In view of the industrial operations at high temperatures ($T_m \sim 103°C$), thermostable α-amylases specifically from the Bacillus genus have attracted greater attention in modern industrial practices (Pandey et al., 2000; Nielsen and Brochert, 2004; Roy et al., 2013; Park et al., 2014). *Bacillus licheniformis* α-amylase (BLA) has been the preferred enzyme over other α-amylases in the starch processing industry involving a high operational temperature (Janecek and Balaz, 1992).

2.2   Isolation and purification

α-Amylases are widely distributed in nature and have been isolated from various sources such as fungi, bacteria, plants and animals. Among the microorganisms, *Bacillus sp*. are the most common sources for α-amylases (Table 2.1). *Bacillus amyloliquefaciens* (BAA) and *Bacillus licheniformis* (BLA) from *Bacillus sp* and *Aspergillus oryzae, Aspergillus niger and Aspergillus awamori* from *Aspergillus sp* (Table 2.1), have been frequently used for the commercial production of the enzyme (Sundram and Murty, 2014). Production of α-amylases is usually determined by the strain of the bacterial species, medium composition and culture conditions (Lin et al., 1998; Okolo et al., 2000). Different techniques of fermentation such as solid-state fermentation, submerged fermentation and batch and fed batch fermentation have been employed to produce α-amylases. Solid-state fermentation is preferred due to its simplicity and similarity to the natural growth conditions of the organism (Kunamneni et al., 2005; Sun et al., 2010).

Table 2.2 shows different purification strategies, which have been employed for α-amylases from *Bacillus* species. Initially, precipitation with ethanol or acetone is carried out to obtain the crude enzyme preparation, which is then subjected to various chromatographic procedures such as gel chromatography, ion exchange chromatography or hydrophobic chromatography. Hamilton *et al.* (1999) have used affinity purification employing α-Cyclodextrin-Sepharose 6B chromatography to prurify α-amylases with high purification fold.

Table 2.1   α-Amylase producing microorganisms.

Microorganism	Reference
Fungi	
Aspergillus awamori KT-11	Matsubara et al. (2004)
Aspergillus ficum	Hayashida & Teramoto (1986)
Aspergillus niger AM07	Omemu et al. (2005)
Aspergillus oryzae VB6	Joel and Bhima (2012)
Streptomyces sp. No 4.	Primarini & Ohta (2000)
Bacteria	
Anoxybacillus contaminas	Lefuji et al. (1996)
Bacillus amyloliquefaciens	Demirkan et al. (2005)
Bacillus licheniformis	Arasaratnam & Balasubramaniam (1992)
Bacillus sp. IMD 434	Hamilton et al. (1999a)
Bacillus sp. IMD 435	Hamilton et al. (1999b)
Bacillus sp. TS-23	Lin et al. (1998)
Bacillus stearothermophilus	Kim et al. (1989)
Bacillus subtilitis 65	Hayashida et al. (1988)
Cytophaga sp.	Jeang et al. (2002)
Streptococcus bovis 148	Satoh et al. (1997)

Table 2.2   Production of α-amylase from Bacillus species.

Microorganism	Purification strategy	Purification fold	Yield (%)	Reference
Bacillus sp. IMD 370	Ethanol precitation ↓ DEAE-BioGel A chromatography ↓ Superose 12 gel chromatography	104.3	14.9	Mctigue et al. (1995)
Bacillus sp. TS-23	Raw starch adsorption ↓ Sephacryl S-100 HR gel chromatography	708.5	13.2	Lin et al.(1988
Bacillus sp. IMD 434	α-Cyclodextrin-Sepharose 6B chromatography	375	65	Hamilton et al. (1988)
Bacillus sp. IMD 434	Acetone precipitation ↓ Resource Q column chromatography ↓ Phenyl-Sepharose chromatography	266	10	Hamilton et al. (1999a)
Bacillus sp. IMD 435	α-Cyclodextrin-Sepharose 6B chromatography	774	65	Hamilton et al. (1999b)
Bacillus licheniformis NHI	40-60% $(NH_4)_2SO_4$ fractionation ↓ Sephadex G-100 gel chromatography ↓ Sepharose mono Q chromatography	3.08	15.9	Hmidet et al. (2008)

	70% $(NH_4)_2SO_4$ fractionation	187.1	19.5	Liu et al. (2008)
	↓			
Bacillus licheniformis	DEAE-Sepharose chromatography			
	↓			
	Sephadex G-75 gel chromatography			
Bacillus sp. YX-1	60% $(NH_4)_2SO_4$ fractionation	34	6.6	Liu & Xu (2008)
	↓			
	DEAE-Sepharose chromatography			
	↓			
	Sephadex G-75 gel chromatography			

2.3   Physicochemical properties

As shown in Table 2.3, techniques of sedimentation equilibrium and SDS-PAGE have yielded different values of the molecular weight of BLA, being 48,700 Da and 58,000 Da, respectively (Chiang et al., 1979; Damodara Rao et al., 2002). However, a low value of the molecular weight (22, 500 Da) has been reported on the basis of gel filtration results (Saito, 1973). Such discrepancy in the molecular weight obtained with gel filtration data can be attributed to the possible interaction of BLA with the gel matrix (Kruger and Lineback, 1987). Dynamic light scattering method has produced a value of 3.20 nm for the Stokes radius of BLA (Fitter and Haber-Pohlmeier, 2004). BLA has been characterized as a neutral protein on the basis of its isoelectric point (7.18), obtained from isoelectric focusing (Esteve-Romero et al., 1996). However, a value of 6.0 has been found for the isoelectric point using the charge ladder technique (Shaw et al., 2008). BLA shows maximum activity at pH 6.0 (Endo, 1999) and posseses high termostability as reflected from its T_m value, 103°C (Fitter and Haber-Pohlmeier, 2004). About 26% helical structure and 24% β-structure constitute the secondary structures of BLA (PDB entry code1BLI).

2.4   Structural organization

2.4.1   Amino acid composition

BLA is a single polypeptide chain, consisting of 483 amino acid residues (PDB entry code 1BLI). As shown in Table 2.4, the total number of acidic amino residues (61) is slightly lower than the total number of basic amino acid residues (73). Although BLA lacks cysteine residue, but the enzyme is characterized by the abundance of 17 tryptophan residues. Presence of 31 tyrosine residues further adds to its absorptivity.

Table 2.3   Physicochemical properties of *Bacillus licheniformis* α- amylase.

Property	Value	Reference
Molecular mass		
- Gel filtration	22, 500 Da	Saito (1973)
- Sedimentation equilibrium	48, 700 Da	Chiang et al. (1979)
- SDS-PAGE	58, 000 Da	Damodara Rao et al. (2002)
Stokes radius		
- Dynamic light scattering	3.2 nm	Fitter & Haber- Pohlmeier (2004)
Isoelectric point		
- Isoelectric focusing	7.18	Esteve-Romero et al. (1996)
- Charge ladder	6.00	Shaw et al. (2008)
Melting temperature (T_m)	103 °C	Fitter & Haber-Pohlmeier (2004)
pH optimum	6.0	Endo (1988)
Secondary structures		
- Helices (α- and 3_{10})	26 %	PDB entry code 1BLI
- β-forms	24 %	PDB entry code 1BLI

Table 2.4   Amino acid composition of *Bacillus licheniformis* α-amylase.*

Amino acid	No. of residues
Glycine	46 (45)
Alanine	35
Valine	32
Leucine	29 (28)
Isoleucine	20
Serine	27 (26)
Threonine	27
Proline	15
Aspartic acid	37
Glutamic acid	24 (25)
Asparagine	23 (25)
Glutamine	19 (20)
Histidine	24
Lysine	28
Arginine	21 (22)
Phenylalanine	21 (20)
Tyrosine	31 (30)
Tryptophan	17
Methionine	7
Total	**483**

*PDB entry code 1BLI

The number of residues in brackets show the variations in the number of residues obtained from cDNA (Yuuki et al., 1985).

2.4.2 Primary structure

Figure 2.1 shows the primary structure of BLA, which is arranged in the form of three domains, namely A, B and C without any disulfide linkage (Machius et al., 1995). Domain A (N-terminal domain) is the most preserved domain in various α-amylases. It consists of residues 1-110 and 203-396 in the primary sequence (Machius et al., 1995). Domain B, which is least similar region of BLA with higher degree of structural complexity is comprised of residues, 111-121 and 133-140 (Machius et al., 1998). A stretch of residues 393-483 forms domain C, which is well-conserved among different α-amylases with the exception of barley α-amylase (Kadziola et al., 1994).

2.4.3 Three-dimensional structure

Figure 2.2 shows the three-dimensional structures of various α-amylases. Most of them consist of a monomer with three domains (domains A, B and C). Domain A forms the central part as β/α-barrel. Domain B along with the central domain A constitute the substrate binding cleft while domain C is positioned opposite to the central β/α-barrel. These enzymes show the presence of at least one conserved calcium binding site (Violet and Meunier, 1989; Fitter et al., 2001; Nielsen et al., 2003).

Domain B, which is the least homologous in different α-amylases is formed from six loosely-connected and twisted antiparallel β sheets and protrudes from domain A as a hump (Machius et al., 1995). Figure 2.3 shows the possible hydrogen bonding pattern in domain B of BLA, which is responsible for the stabilization of β sheet structures.
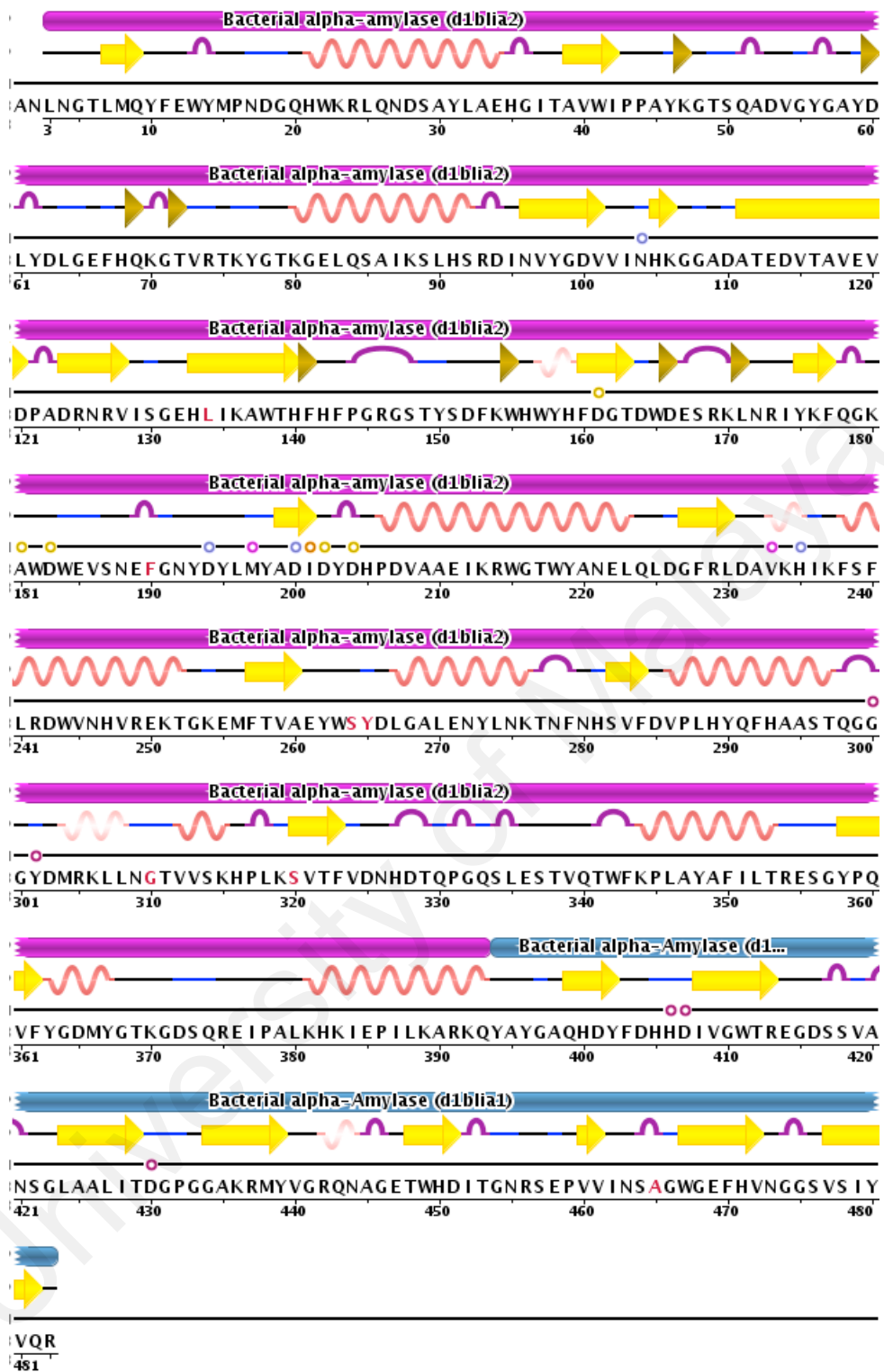
Figure 2.1 Primary structure of BLA. The complete amino acid sequence corresponding to mature BLA is adapted from Protein Data Bank (entry code 1BLI). The position of α-helices and β-sheets as determined from BLA crystal structure (Machius *et al*., 1998) are indicated by spirals and arrows respectively, coloured in red and yellow. dblia1 (dark blue) and dblia2 (purple) refer to glycosyl hydrolase domain and TIM β/α barrel, repectively.
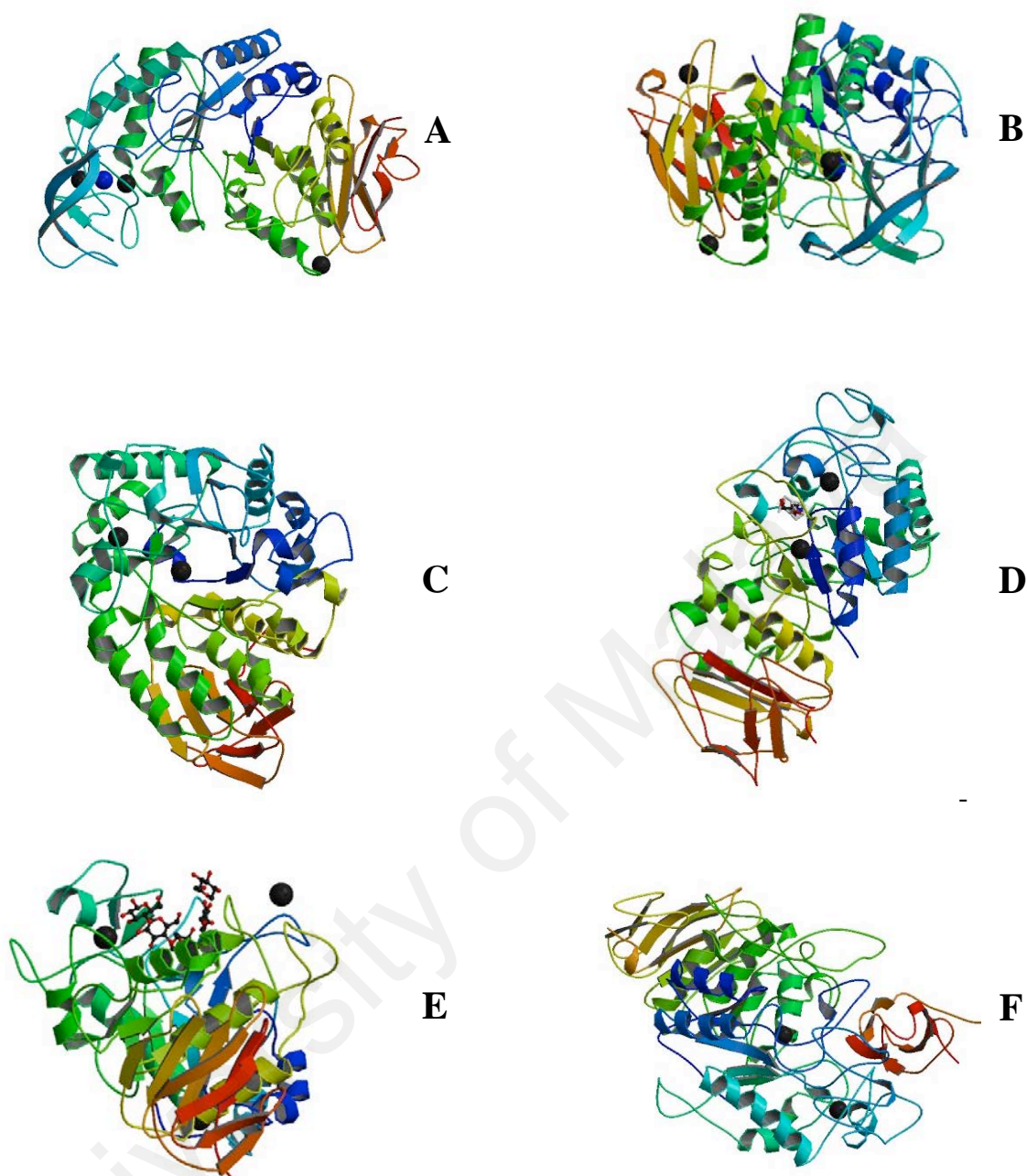
Figure 2.2 Three-dimensional structures of various α-amylases. (A) α-amylase from *Bacillus licheniformis* (PDB entry code 1BLI), (B) α-amylase from *Bacillus amyloliquefaciens* (PDB entry code 3BH4), (C) α-amylase from *Aspergillus oryzae* (TAKA) (PDB entry code 6TAA), (D) α-amylase from *Alteramonas haloplanctis* complexed with Tris (PDB entry code 1AQM), (E) α-amylase from *Bacillus subtilis* complexed with maltopentaose (PDB entry code 1BAG), (F) α-amylase from porcine pancrease (PPA) complexed with the proteinaceous inhibitor Tendamistat (PDB entry code 1BVN).
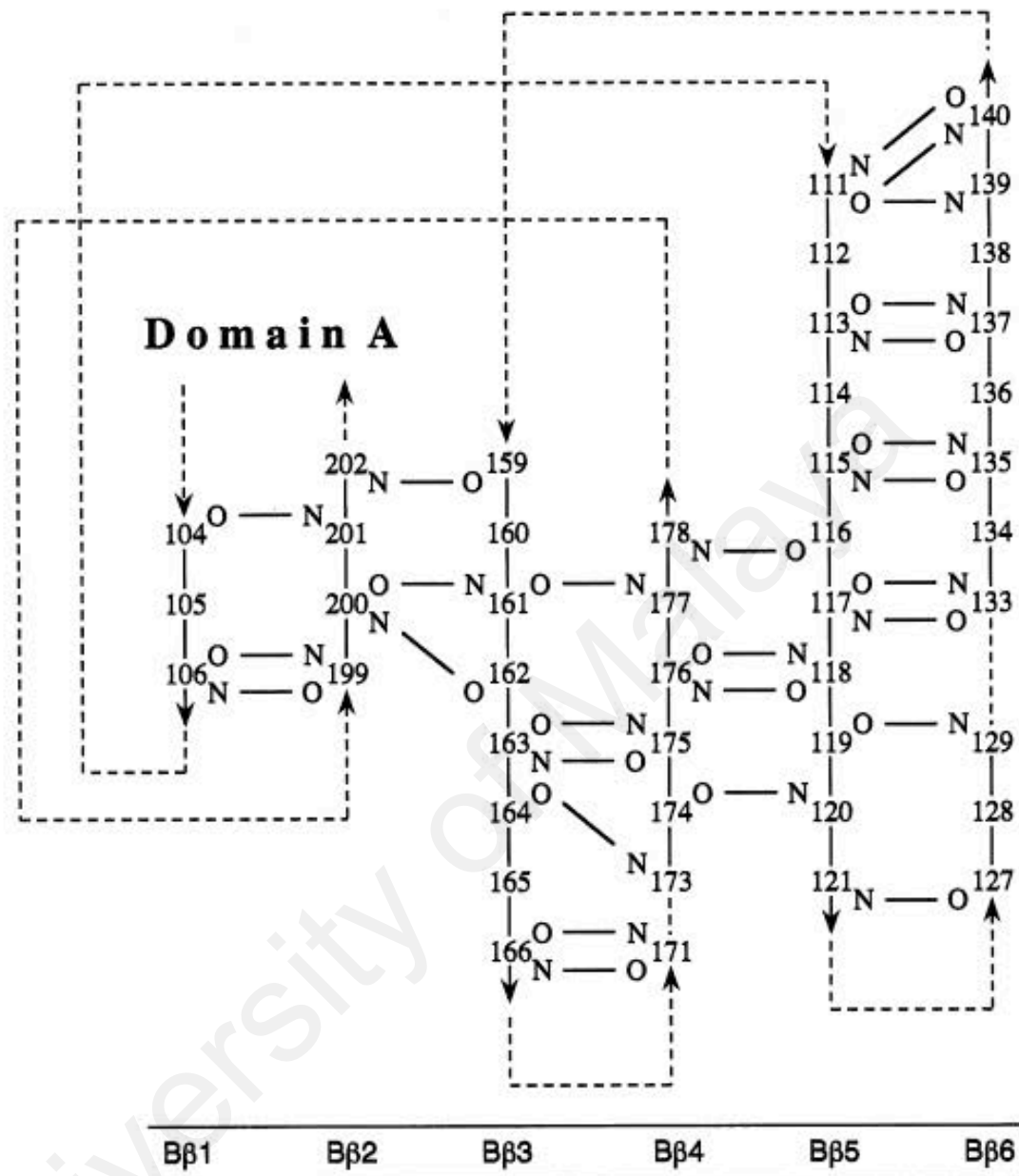
Figure 2.3 A representation of all β structures in domain B of BLA.

(Reprinted from ***Journal of Molecular Biology***, **246**, Machius, M., Wiegand, G. and Huber, R., Crystal structure of calcium-depleted *Bacillus licheniformis* α-amylase at 2.2 Å resolution, 545–559 (1995), with permission from Elsevier.)

2.4.4 Calcium binding site

BLA contains three calcium binding sites, as shown in Figure 2.4. The first site (Ca I) is located at the interface between domain B and the C-terminus of the central barrel. The second calcium binding site (Ca II) is also located in close proximity to Ca I in domain B of BLA. The third calcium binding site (Ca III) lies at the interface between domains A and C (Figure 2.4) (Machius et al., 1998). Table 2.5 shows the distance between the metal ions in BLA and its ligand. The coordination geometry of Cal III differs from Ca I and Cal II in being the position trans to the bidentate aspartate, occupied by a water molecule (Machius et al., 1998).

2.5 Stability

The stability of α-amylases has been extensively studied due to their importance in the industrial processes. The protein stability is widely reflected from its tolerance towards several factors, such as temperature, pH and chemical denaturants (Fagain and Kennedy, 1991; Fagain, 1995).

2.5.1 pH

The stable pH range differs in various α-amylases. For example, *Thermus filiformis* α-amylases remain active in the pH range, of 4.0–8.0 (Egas et al., 1988), whereas *Bacillus subtilitis* α-amylases are stable in the pH range, 4.0–9.0 (Nagarajan et al., 2006). The stability of BLA has been found to be in the pH range from 7.0 to 9.0 (Krishnan and Chandran, 1983). Furthermore, BLA has been shown to possess an activity of 95 % and 50 % at pH 10.0 and pH 3.0, respectively (Krishnan and Chandran, 1983). α-Amylases from *Clostridium acetobutylicum* and *Bacillus sp*. KR-810, have shown stability under pH range, 3.0–5.0 (Paquet et al., 1991)
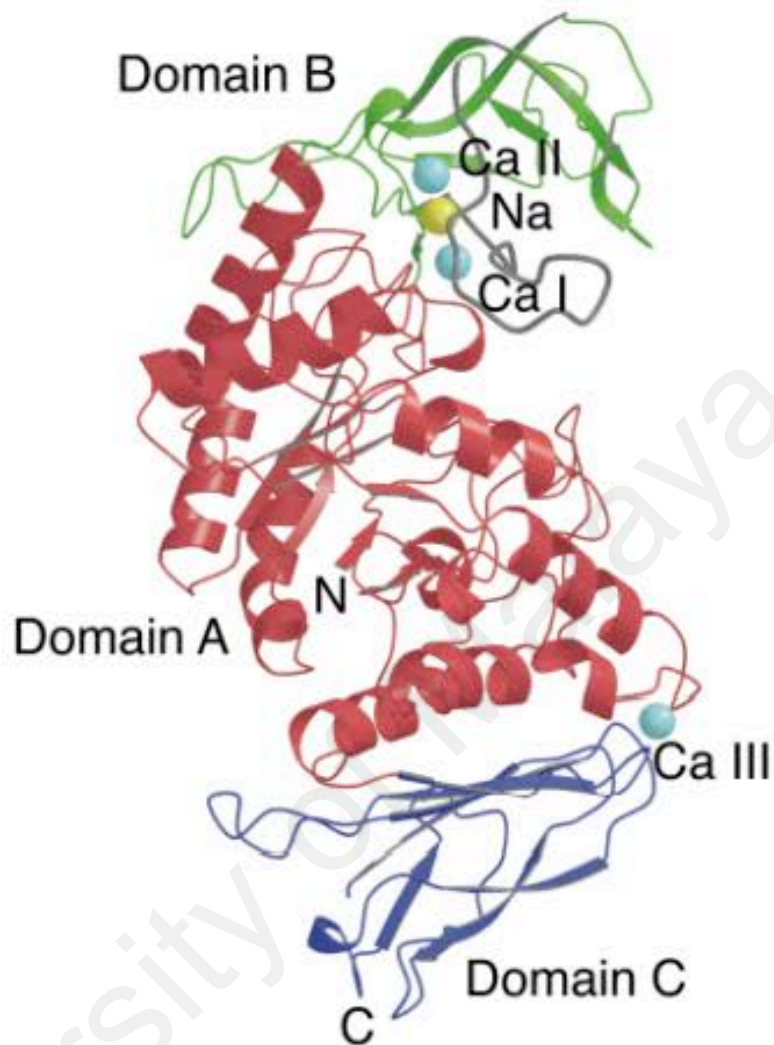
Figure 2.4 Tertiary structure of *Bacillus licheniformis* α-amylase. The calcium and sodium ions bound to the protein in its native form are shown. Domain A, shown in red, is a β/α TIM barrel. Doman B is colored in green and domain C in blue. The three calcium ions are shown in blue and the sodium ions is shown in gold.

(Reprinted from ***Structure***, **6**(3), Machius, M., Declerck, N., Huber, R. and Wiegand, R. Activation of *Bacillus licheniformis* α-amylase through a disorder →order transition of the substrate-binding site mediatedly by a calcium-sodium-calcium metal triad, 281-292 (1998), with permission from Elsevier.)

Table 2.5   Distances between the metal ions in *Bacillus licheniformis* α-amylase and its ligands.*

Metal ion	Ligand	Distance (Å)
Calcium I		
	Asn104 OD1	2.4
	Asp194 O	2.4
	Asp194 OD1	2.5
	Asp200 OD1	2.4
	Asp200 OD2	3.0
	His235 O	2.4
	Wat	2.6
Calcium II		
	Asp161 OD1	2.6
	Asp161 OD2	2.6
	Ala181 O	2.4
	Asp183 OD1	2.4
	Asp202 OD2	2.5
	Asp204 OD1	2.6
	Wat	2.6
Calcium III		
	Gly300 O	2.6
	Tyr302 O	2.3
	His406 O	2.6
	Asp407 OD2	2.3
	Asp430 OD1	2.6
	Asp430 OD2	2.6
	Wat	2.9
Sodium		
	Asp161 OD1	2.4
	Asp183 OD2	2.7
	Asp194 OD1	3.1
	Asp194 OD2	2.5
	Asp200 OD2	2.4
	I1e201 O	2.5

(Reprinted from ***Structure***, **6**(3), Machius, M., Declerck, N., Huber, R. and Wiegand, R. Activation of *Bacillus licheniformis* α-amylase through a disorder →order transition of the substrate-binding site mediatedly by a calcium-sodium-calcium metal triad, 281-292 (1998), with permission from Elsevier.)

2.5.2 Temperature

The optimum temperature for most of α-amylases has been found to lie in the range, 40–65 °C (Sun et al., 2007). BLA possesses an optimum temperature of 90 °C (Fitter et al., 2001). However, this thermostability is affected by the presence of calcium ions. Thermal stability of various α-amylases has been studied using calorimetry and spectroscopic techniques. The half life ($T_{1/2}$) of BLA has been shown to be much longer (270 min) compared to *Bacillus amyloliquefaciens* α-amylase (BAA) (2 min) and *Bacillus stearothermophilus* α-amylase BStA (50 min) under similar conditions of 90 °C, pH 6.5 (Table 1.1) (Declerck et al., 2002).

2.5.3 Chemical denaturants

Several studies on GdnHCl-denaturation of BLA have been made to investigate the role of calcium towards BLA stability (Fitter and Habber-Pohlmeier, 2004; Duy and Fitter, 2006; Strucksberg et al., 2007; Tan et al., 2010). GdnHCl-induced structural changes in BLA have been shown at 1.5 M GdnHCl using emission maximum probe. Fully unfolded BLA has been found to remain soluble without any aggregation at 6.0 M GdnHCl (Strucksberg et al., 2007). In the presence of 2 mM CaCl₂, both native and calcium-depleted BLA have shown relatively higher stability against GdnHCl (Tan et al., 2010). Fluorescense quenching studies with potassium iodide have revealed the exposure of a few (8) Trp residues in the partially folded state and GdnHCl denaturation of BAA has been found free from any aggregated forms (Zhang et al., 2009). GdnHCl denaturation of *Bacillus subtilis* α-amylase (BSUA) has been shown to be reversible at pH 7.0, when monitored by intrinsic fluorescence measurements and proteolytic degradation (Haddaoui et al., 1997). The first renaturation step depicting conversion

from a totally denatured state to a partially-structured state of the protein within 1 second. This intermediate has been found resistant towards proteolytic degradation and requires calcium for its transformation into native state (Haddaoui et al., 1997)

Aqueous, ready-to-use enzyme solutions are preferred for industrial applications. However, most of these are not stable in solution for a long period. Hence, additives in enzyme formulation such as metal ions (Brennan et al., 2003; Wu et al., 2015) and other stabilizing agents including buffer components are used to stabilize the enzyme (Ulrika et al., 2004). Buffers, such as cacodylate, MES, HEPES, Tris and phosphate buffers have been found to produce differential effects with respect to deoxynucleotidyl transferase-catalyzed polymerization of deoxynucleoside triphosphates (Ugwu and Apte, 2004). Therefore, the effect of buffer composition on the stability of BLA was studied. The role of calcium in the stability against GdnHCl denaturation of native and calcium depleted BLAs in the presence of different buffers was also investigated.

MATERIALS AND METHODS

3. MATERIALS AND METHODS

3.1 Materials

3.1.1 Protein

α-Amylase from *Bacillus licheniformis* (BLA) (93−100% by SDS-PAGE) (Lot No. 018K7018V) was purchased from Sigma-Aldrich Co., USA. The commercial BLA preparation (partially saturated with calcium) was used as such in these studies without any further treatment and is termed as BLA / native BLA.

3.1.2 Reagents used in gel chromatography

Sephacryl S-200 HR, MW range 5-250 kDa (lot 116K0771) and blue dextran (lot 066K1083) were obtained from Sigma-Aldrich Co., USA. L-Tyrosine (lot 6380446) was supplied by Merck, Germany.

3.1.3 Reagents used in denaturation experiments

Guanidine hydrochloride (GdnHCl) ($\geq$99 % pure), 3-(N-morpholino)propanesulfonic acid sodium salt (MOPS), 4-(2-hydroxyethyl)piperazine-1-ethanesulfonic acid sodium salt (HEPES), ethylene glycol-bis (2-aminoethylether)-N,N,N',N'-tetraacetic acid (EGTA), sodium dihydrogen phosphate and disodium hydrogen phosphate were purchased from Sigma-Aldrich Co., USA. Tris (hydroxymethyl)aminomethane was obtained from AMRESCO, USA. Hydrochloride acid (HCl) was the product of Systerm, Malaysia.

3.1.4 Miscellaneous

Standard buffers of pH 7.0 and pH 10.0 as well as dialysis tubing of 27 mm diameter were purchased from Sigma-Aldrich Co., USA. Parafilm 'M' was the product of Bemis Flexible Packaging, USA. PVDF hydrophilic membrane (0.45µm) Millex HV syringe driven filter units were obtained from Millipore Corporation, Ireland. Cellulose nitrate membrane filters (0.22 and 0.45 µm pore size) were supplied by Merck Milipore, Germany.

All glass distilled water or Ultrapure (Type 1) water produced by Milli-Q water purification system (Merck Millipore, Germany) was used throughout these studies. All experiments were carried out at room temperature (~ 25°C).

3.2 Methods

3.2.1 pH measurements

pH measurements were made on Delta 320 pH meter (Mettler-Toledo GmbH, Switzerland) using a HA405-K2/120 combination electrode. The pH meter was routinely calibrated at room temperature with standard buffers of pH 7.0 and pH 10.0 for pH measurements in the neutral and alkaline pH ranges, respectively.

3.2.2 Preparation of calcium-depleted BLA

The method described by Nazmi *et al* (2006) was used to prepare calcium-depleted BLA (Ca-depleted BLA) with slight modification. Ca-depleted BLA preparation was made by dialyzing the commercial BLA solution against 150 mM Tris/20 mM EGTA buffer, pH 7.5 overnight with three changes in the same buffer. Removal of EGTA from the dialyzed sample was performed by dialysis against the desired buffer (50 mM sodium phosphate, 150 mM Tris-HCl, 150 mM HEPES and

150 mM MOPS) of pH 7.5. Dialysis was carried out at 4°C for 24 h and the dialyzed protein solutions were stored in plastic bottles in order keep them free from Ca^{2+} contamination.

3.2.3 Preparation of the stock protein solutions

BLA (native and Ca-depleted) stock solutions were prepared by dissolving a fixed amount of the protein in a fixed volume of the respective buffers (50 mM sodium phosphate, 150 mM Tris-HCl, 150 mM HEPES and 150 mM MOPS) of pH 7.5. All the protein solutions prepared in different buffers were filtered using PVDF membrane (0.45 μm) syringe-driven Millipore filter units before concentration measurements. The protein stock solutions were stored in plastic bottles at 4°C and were used within 2 weeks.

3.2.4 Determination of protein concentration

Protein concentration of the stock protein solutions was determined spectrophotometrically using a molar extinction coefficient of 139,690 $M^{-1}cm^{-1}$ at 280 nm (Nazmi et al., 2007).

3.2.5 Absorption spectroscopy

Absorption measurements were carried out on a Shimadzu double-beam spectrophotometer (Shimadzu Corp., Japan), model UV-2450, using quartz cuvettes of 1 cm path length. Scattering corrections, if required, were made by extrapolation of the absorbance values in the wavelength range, 360−340 nm to the desired wavelength, as described elsewhere (Tayyab and Qasim, 1986).

3.2.6   Fluorescence spectroscopy

Fluorescence spectra of different protein solutions were obtained on a Hitachi fluorescence spectrophotometer (Hitachi Corp., Japan), model F-2500, equipped with a thermostatically-regulated cell holder. Occasionally, fluorescence measurements were also performed on Jasco spectrofluorometer (Jasco International Co., Japan), model FP-6500. The excitation and emission slits were fixed at 10 nm each, while the scan speed was maintained at 500 nm/min.

The fluorescence spectra of the protein solutions (0.1 µM) taken in 1 cm path length quartz cuvette were recorded in the wavelength range, 305–400 nm after exciting the protein solutions at 280 nm. Values of the fluorescence intensity were plotted against wavelength to get the fluorescence spectra.

3.2.7   Circular dichroism spectroscopy

Circular dichroism (CD) spectral measurements of different BLA preparations were carried out in the far-UV range (200–250 nm) on a Jasco spectropolarimeter (Jasco International Co., Japan), model J-815, attached to a Jasco PTC-423S/15 Peltier-type temperature controller under constant nitrogen flow. The CD facilities were kindly provided by the Malaysian Genome Institute, Bangi, Selangor, Malaysia. After calibrating the instrument with (+)-10-camphorsulfonic acid, spectral measurements were recorded at 25°C using a scan speed of 100 nm/min and a response time of 1 sec. A protein concentration of 1.7 µM in a 1 mm path length cuvette was used for spectral measurements. Each spectrum was the average of three scans and was corrected with the suitable blank.

The CD values were transformed into mean residue ellipticity (MRE) in deg.cm^2.dmol^{-1} using the following equation:

$$MRE = \theta_{obs} \times (MRW / 10 \times c \times l) \qquad (1)$$

where 'θ_{obs}' is the observed ellipticity in millidegrees; 'MRW' is the mean residue weight, obtained by dividing the molecular weight of the protein (55,200 Da) with the total number of amino acid residues (483) in the protein (Yuuki et al., 1985); 'c' is the concentration of protein in mg/mL and 'l' is the optical path length in centimeters. The MRE values, thus obtained were plotted against wavelength to get the far-UV CD spectra.

3.2.8   Ultraviolet difference spectroscopy

The ultraviolet (UV) absorption spectra of different protein solutions were recorded in the wavelength range, 250-305 nm, using a protein concentration of 5.2 µM in 1 cm quartz cells. UV difference spectra were obtained by subtracting the absorbance values of the native protein from the absorbance values of the GdnHCl-denatured BLA at each wavelength. These values were transformed into differential extinction coefficient and plotted against wavelength.

3.2.9   Guanidine hydrochloride denaturation

3.2.9.1 Preparation of guanidine hydrochloride stock solutions

The stock guanidine hydrochloride (GdnHCl) solutions were prepared in different buffers, following the procedure described by Pace *et al* (1989) and its concentration was determined from the data of Nozaki (1972).

The weight fraction denaturant in the solution (W) was calculated using the following formula:

$$W = \frac{\text{Weight of solid GdnHCl (g)}}{\text{Weight of GdnHCl solution (g)}} \qquad (2)$$

The ratio of the density of the solution to the density of water (d/d_0) of the GdnHCl solution was calculated with the help of the value of 'W', using Eq. 3:

$$d/d_0 = 1 + 0.271\ W + 0.033\ W^2 \qquad (3)$$

The volume of the GdnHCl solution, V was obtained by substituting the value of d/d_0 in the given formula: $\qquad (4)$

$$V\ (mL) = \frac{\text{Weight of GdnHCl solution (g)}}{d/d_0}$$

The concentration of the stock GdnHCl solution was determined with the help of the following Eq. 5:

$$\text{Stock GdnHCl concentration (M)} = \frac{\text{Weight of solid GdnHCl (g)}}{MW \times V\ (L)} \qquad (5)$$

where MW is the molecular weight of GdnHCl (95.53 g/mole).

3.2.9.2 Guanidine hydrochloride denaturation experiments

GdnHCl-denaturation experiments were carried out following the procedure described by Muzammil *et al* (2000). Different buffers (0.05 M sodium phosphate, 0.15 M Tris-HCl, 0.15 M HEPES and 0.15 M MOPS) of similar pH value (7.5) were used to perform GdnHCl-denaturation experiments. All solutions for denaturation experiments were prepared in the same buffer.

Increasing volumes of the buffer were added first to 0.5 ml of the stock protein solution (native / Ca-depleted BLA) taken in different tubes, followed by the addition of different volumes of the stock (7 M) GdnHCl solution to obtain the desired concentration of the denaturant. The final protein concentration used was 0.1 μM and 1.7 μM for fluorescence and CD spectral measurements, respectively. The tubes containing final reaction mixture (5.0 mL) were incubated for 12 h at room temperature (25°C) to achieve equilibrium before spectral measurements. Values of the MRE and the fluorescence intensity were transformed into the relative MRE and the relative fluorescence intensity in the same way as described earlier (Tan et al., 2010) and the data were plotted against GdnHCl concentration. These values at different GdnHCl concentrations were obtained by taking the MRE_{222nm} or the fluorescence intensity at 337 nm values of BLA in the absence of GdnHCl as 100%.

3.2.10 Gel chromatography

AKTAprime plus (GE Healthcare, UK), equipped with a pre-packed Sephacryl S-200 HR column (Tricorn Column, GE Healthcare, UK) (1.0×30 cm) was used to study the effect of GdnHCl on BLA aggregation.

The void volume, V_0 of the column was determined by injecting 1 mL of the blue dextran solution (5 mg/mL) prepared in the same buffer. GdnHCl-denatured BLA samples were prepared by incubating BLA in the desired GdnHCl concentration for 12 h at room temperature. The buffer contained the same concentration of GdnHCl for the chromatographic elution of GdnHCl-denatured BLA samples. Gel chromatography of different BLA samples (native BLA, 3 M and 6 M GdnHCl-denatured BLAs) was performed in various buffers (0.05 M sodium phosphate, 0.15 M Tris-HCl, 0.15 M HEPES and 0.15 M MOPS) of the similar pH value (7.5) in the same way. A sample size of 1.25−1.50 mg/500 µL was used to inject various samples into the column and the elution was performed with a flow rate of 0.2 mL/min. Each experiment was repeated 2-4 times to check reproducibility.

Flow Chart Of The Research Flow
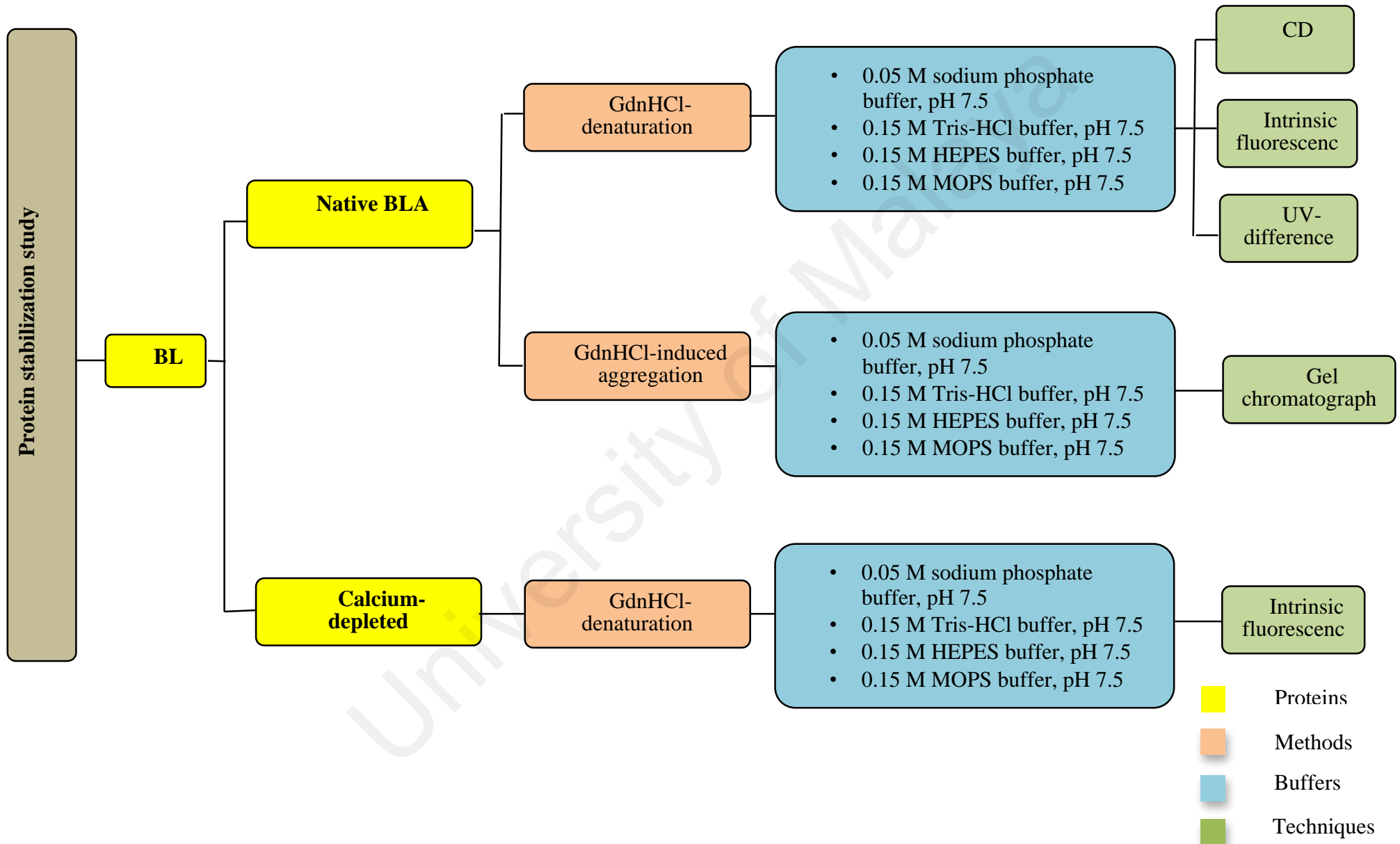
RESULTS AND DISCUSSION

4. RESULTS AND DISCUSSION

4.1 Effect of buffer composition on *guanidine hydrochloride* denaturation of BLA

GdnHCl denaturation of BLA was studied in different buffers using CD, fluorescence and UV difference spectral signals as probes.

4.1.1 Circular dichroism

The effect of increasing GdnHCl concentrations on the secondary structural characteristics of BLA was studied using far-UV CD spectroscopy. Figure 4.1 shows the far-UV CD spectra of BLA in the absence and the presence of increasing GdnHCl concentrations, as obtained in 0.05 M sodium phosphate buffer, pH 7.5. As evident from the figure, the far-UV CD spectrum of the native state of BLA was characterized by the presence of two minima around 208 nm and 222 nm, characteristics of the α-helical structure (Asghari et al., 2004; Shaw et al., 2008). This was in agreement with the presence of 26 % α-helical content in BLA (PDB entry code 1BLI). The complete CD spectra of BLA could not be obtained in the presence of GdnHCl due to high signal to noise ratio at lower wavelengths. The presence of GdnHCl in the incubation mixture produced successive decrease in the MRE values in a concentration dependent manner. However, a small increase was also noted at higher GdnHCl concentrations. This can be more clearly seen in Figure 4.2, where the relative MRE_{222nm} values are plotted against GdnHCl concentrations. Qualitatively similar far-UV CD spectra were obtained in different buffers. However, significant differences in the CD spectral signal were observed in different buffers at the same GdnHCl concentration.
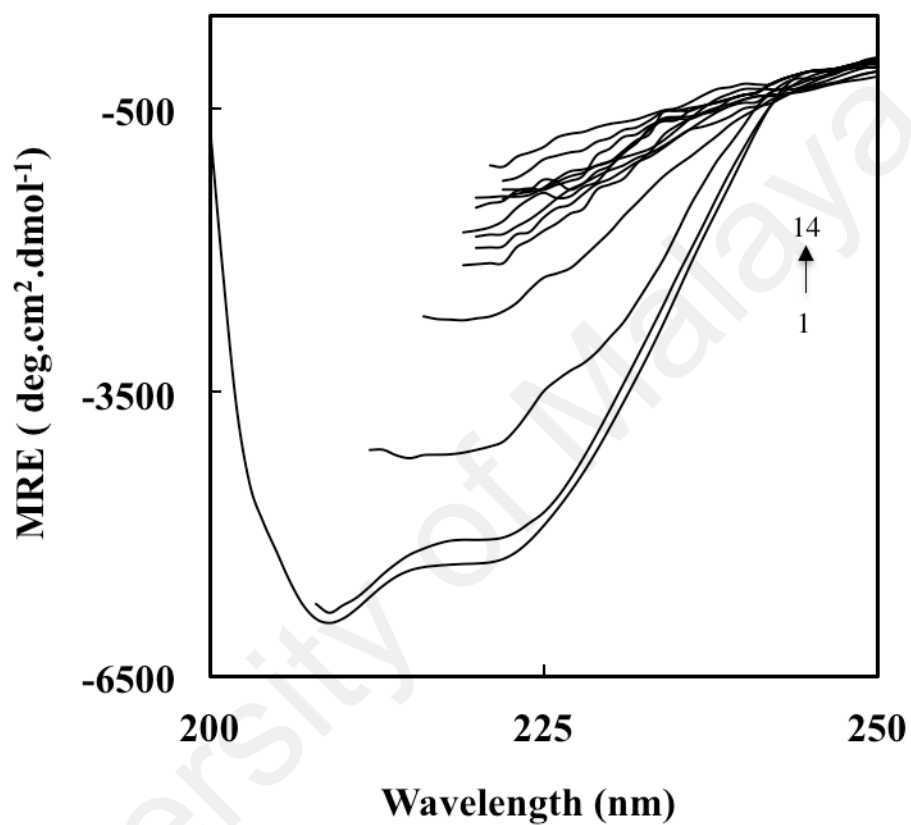
Figure 4.1   Far-UV CD spectra of GdnHCl denaturation of native BLA in 0.05 M sodium phosphate buffer pH 7.5 at 25°C. GdnHCl concentrations from top to bottom were: 0.0, 0.25, 0.5, 1.0, 1.5, 2.0, 6.0, 2.5, 5.5, 5.0, 3.0, 3.5, 4.5 and 4 M GdnHCl respectively.

Figure 4.2 shows GdnHCl-induced denaturation curves of native BLA, as studied by MRE_{222nm} measurements in the presence of different buffers (0.05 M sodium phosphate, 0.15 M Tris-HCl, 0.15 M HEPES and 0.15 M MOPS), pH 7.5. The denaturation curves obtained in these buffers displayed similar patterns, showing an initial decrease in the $-MRE_{222nm}$ value, reaching to a minimum, followed by an increase at higher GdnHCl concentrations. However, quantitative differences were noticed among them. Whereas maximum change in the $-MRE_{222nm}$ signal was observed in the presence of sodium phosphate buffer, smaller variations in the spectral signal were detected in MOPS buffer. More specifically, alterations in the MRE_{222nm} signal followed the order: sodium phosphate > Tris-HCl > HEPES > MOPS buffers. It is worth noting that MRE_{222nm} values could not be collected at lower (< 2.0 M) GdnHCl concentrations in the presence of Tris-HCl buffer due to significant precipitation. This was in agreement to the previous results on GdnHCl denaturation of BLA (Tan et al., 2010).

As evident from Figure 4.2, there was a continuous decrease in the $-MRE_{222nm}$ signal up to 3.0/3.5 M GdnHCl beyond which a continuous increase in the signal was noticed in all buffers. About 75% decrease in the $-MRE_{222nm}$ value was observed at 3.5 M GdnHCl concentration in the presence of sodium phosphate buffer. On the other hand, ~61%, ~33% and ~24% decrease in the $-MRE_{222nm}$ value was detected in the presence of Tris-HCl, HEPES and MOPS buffers, respectively. Being an indicator of the α-helical structure, any decrease in the $-MRE_{222nm}$ value was suggestive of the loss of α-helical structure in BLA (Muzammil et al., 2000), which in turn suggested protein denaturation. Several earlier reports have proposed GdnHCl denaturation of proteins based on the decrease in the $-MRE_{222nm}$ signal (Lai et al., 1997; Fitter et al., 2004; Halim et al., 2013;). Anomalous behavior observed at higher (>4.0M)
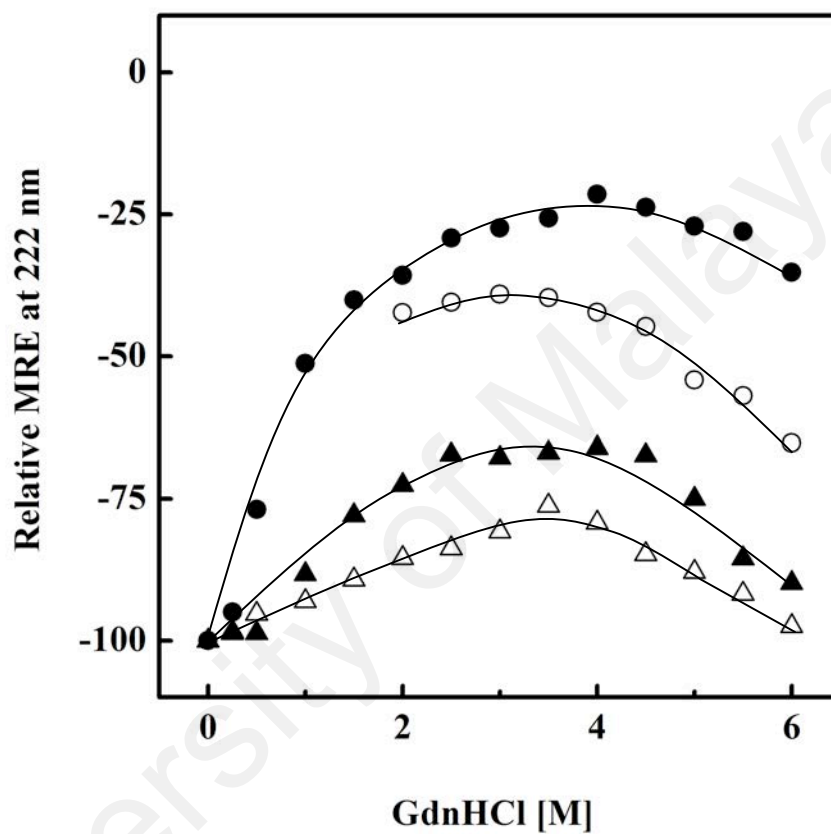
Figure 4.2 GdnHCl denaturation of native BLA in different buffers using MRE measurements at 222 nm. Different buffers used were: 0.05 M sodium phosphate (●); 0.15 M Tris-HCl (○); 0.15 M HEPES (▲) and 0.15 M MOPS (△), of similar ionic strength (0.15) and pH (7.5).

GdnHCl concentrations can be ascribed to protein aggregation due to protein-protein interactions in the unfolded forms. This was not uncommon as Strucksberg *et al* (2007) have also shown similar aggregation of BLA, but at lower GdnHCl concentrations. Such differences can be explained on the basis of different BLA treatments, ionic strength and buffer composition used in an earlier study (Strucksberg et al., 2007).

4.1.2 Intrinsic fluorescence

Tertiary structural alteration of BLA in the presence of increasing GdnHCl concentrations was evaluated by intrinsic fluorescence measurements. Figure 4.3 shows intrinsic fluorescence spectra of BLA in the absence and the presence of increasing GdnHCl concentrations in 0.05 M sodium phosphate buffer, pH 7.5. The intrinsic fluorescence spectrum of the native BLA was characterized by the presence of an emission maximum at 337 nm due to the abundance of Trp residues (Callis, 1997). A significant decrease in the fluorescence intensity was noticed at lower GdnHCl concentrations, followed by a small increase at higher GdnHCl concentrations. The fluorescence spectra of BLA also showed significant shift in the emission maximum upon GdnHCl treatment. The fluorescence spectra, obtained in the presence of Tris-HCl, MOPS and HEPES buffers were qualitatively similar to those obtained in sodium phosphate buffer.

Variations in the relative fluorescence intensity of the native BLA at 337 nm in the presence of increasing GdnHCl concentrations in different buffers are shown in Figure 4.4. A significant decrease in the fluorescence intensity was observed up to 1.5 M GdnHCl, before sloping off in the presence of Tris-HCl, MOPS and HEPES buffers. Whereas, the decrease in the fluorescence intensity continued up to 2.5 M GdnHCl in the presence of sodium phosphate buffer and sloped off thereafter. A comparison of these results, obtained in four different buffers clearly suggested that the effect of

35
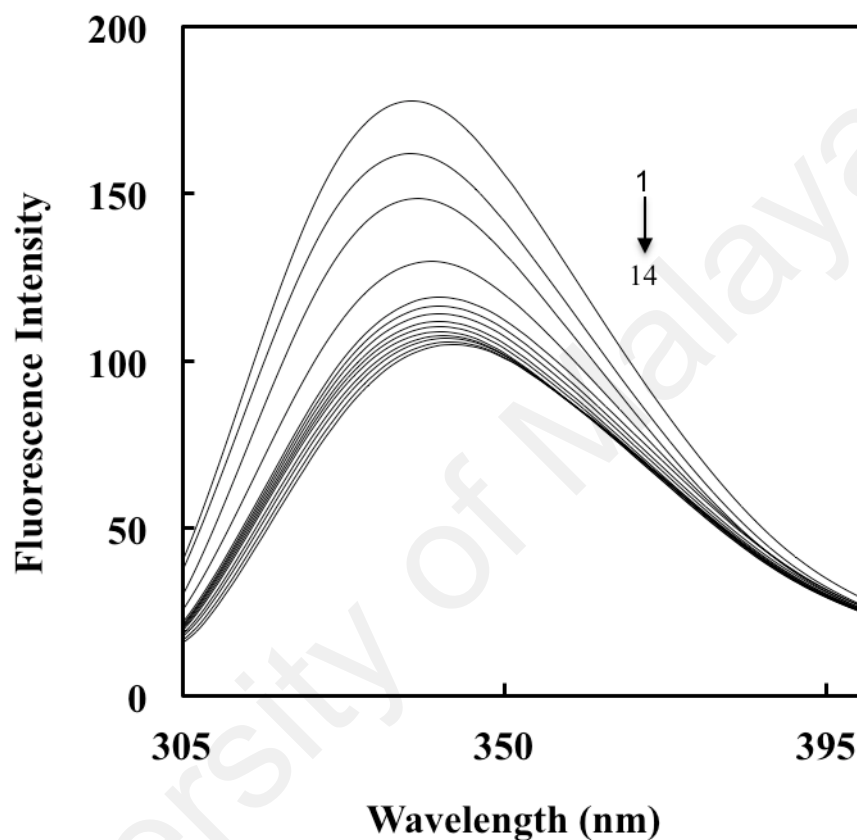
Figure 4.3 Fluorescence spectra of GdnHCl denaturation of native BLA in 0.05 M sodium phosphate buffer, pH 7.5 at 25°C upon excitation at 280 nm. GdnHCl concentrations from top to bottom were: 0, 0.25, 0.5, 1.0, 1.5, 6.0, 5.5, 5.0, 4.5, 4.0, 2.0, 2.5, 3.5 and 3.0 M GdhnHCl respectively.

Figure 4.4 GdnHCl denaturation of native BLA in different buffers using intrinsic fluorescence measurements at 337 nm upon excitation at 280 nm. Different buffers used were: 0.05 M sodium phosphate (●); 0.15 M Tris-HCl (○); 0.15 M HEPES (▲) and 0.15 M MOPS (△), of similar ionic strength (0.15) and pH (7.5).

sodium phosphate buffer was more pronounced showing 48% decrease in the fluorescence intensity at 2.5 M GdnHCl against 27% decrease, observed with Tris-HCl buffer. Interestingly, two other buffer systems *i.e.* HEPES and MOPS showed more or less similar changes in the fluorescence intensity up to 2.5 M GdnHCl concentration. About 15% decrease was observed at 2.5 M GdnHCl, followed by a slow increase up to 6.0 M GdnHCl concentration. BLA has been reported to contain 17 Trp and 30 Tyr residues (Duy et al., 2006), all of which are distributed both in the protein interior and at the surface (Shokri et al., 2006). Therefore, a decrease in the fluorescence intensity in the presence of GdnHCl reflected the exposure of Tyr and Trp residues of BLA to a polar environment, suggesting protein denaturation. A similar decrease in the fluorescence intensity has been reported in many proteins upon GdnHCl treatment (Rashid et al., 2005; Jana et al., 2006; Zhang et al., 2013). As described in the section 3.1.4, anomalous behavior in the fluorescence spectral signal at higher GdnHCl concentrations can be ascribed to BLA aggregation. Effectiveness of buffers in producing GdnHCl-induced changes in the fluorescence intensity followed the similar order (sodium phosphate > Tris-HCl > HEPES > MOPS), as observed with MRE_{222nm} measurements.

Besides showing a decrease in the fluorescence intensity, the fluorescence spectra of BLA also showed a significant shift in the emission maximum upon GdnHCl treatment (Figure 4.3). Such shift in the emission maximum of BLA with increasing GdnHCl concentrations, observed in four different buffers can be clearly seen from Figure 4.5. Sodium phosphate buffer produced the maximum red shift from 337 nm (for native BLA) to 347 nm at 3.5 M GdnHCl beyond which it decreased, reaching to a value of 344 nm at 6.0 M GdnHCl. In an earlier study, an emission maximum of 348 nm was observed with 1.5 M GdnHCl-denatured BLA (Strucksberg et al., 2007). The difference in the GdnHCl concentration needed to produce similar denatured states can be ascribed to the different treatment and buffer composition used in the previous study.

On the other hand, the emission maximum shifted gradually towards higher wavelength up to 2.5 M GdnHCl and remained unchanged thereafter in the remaining three buffers. Whereas 3 nm red shift was observed at 2.5 M GdnHCl with Tris and HEPES buffers, only 2 nm red shift was produced in MOPS buffer. Red shift in the emission maximum, observed with increasing GdnHCl concentrations was suggestive of the transfer of Tyr and Trp residues from nonpolar to polar environment as a result of protein denaturation. These results were similar to those shown in Figures 4.2 and 4.4 in terms of greater effectiveness of the phosphate buffer, followed by Tris-HCl, HEPES and MOPS buffer systems. Significant reversal in the shift of the emission maximum, observed at higher GdnHCl concentrations indicated placement of Tyr and Trp residues in smaller hydrophobic pockets. This seems justifiable from the primary sequence of BLA, where most of the neighboring residues around Trp and Tyr are hydrophobic in nature (Declerck et al., 2002) It seems plausible to assume the formation of hydrophobic clusters in the denatured BLA, which might have led to the burial of Tyr and Trp residues into nonpolar environment, leading to reversal of the fluorescence intensity signal and its emission maximum (Machius et al., 2003). Furthermore, significant aggregation of BLA molecules was also observed at higher GdnHCl concentrations (section 4.2), which might have also contributed to such spectral behavior.

Smaller fluctuations in the fluorescence signals (fluorescence intensity and emission maximum) obtained with HEPES and MOPS buffers may also be viewed as stabilizing effect of these buffers towards BLA against GdnHCl denaturation. This seems justifiable in view of the hydrophobic environment produced by piperazine ring of HEPES and morpholine ring of MOPS around surface residues of BLA. Ternary metal binding site in BLA has been suggested as one of the major nucleation sites for unfolding (Machius et al., 2003), which might be stabilized by these buffers. Alternatively, these buffers might have created nonpolar environment around protein
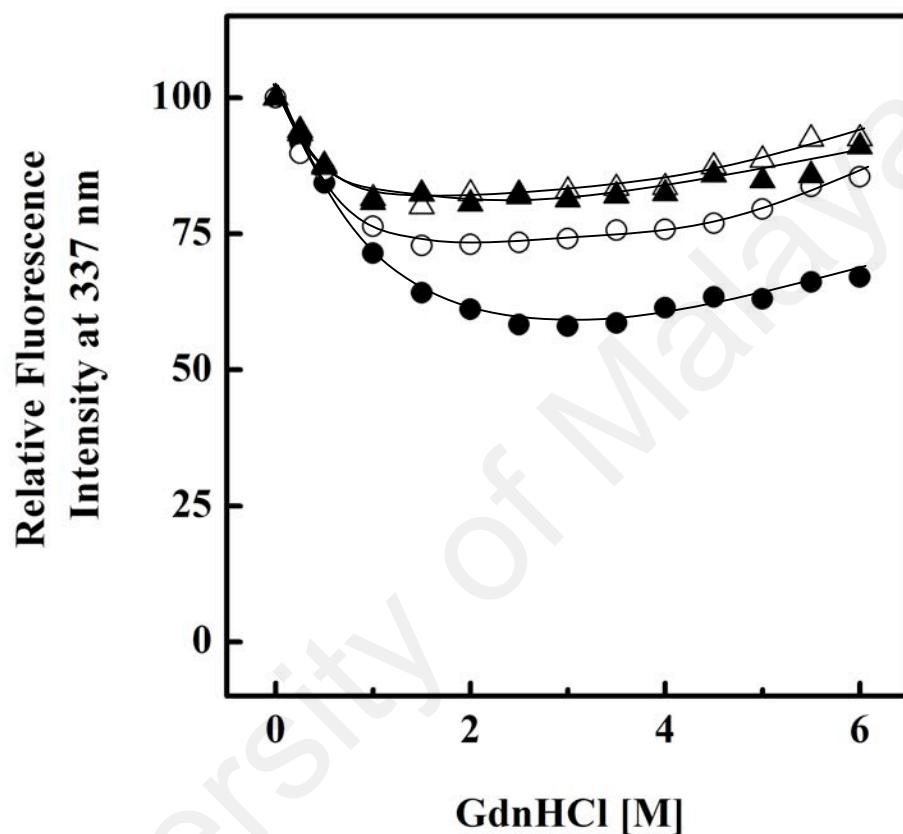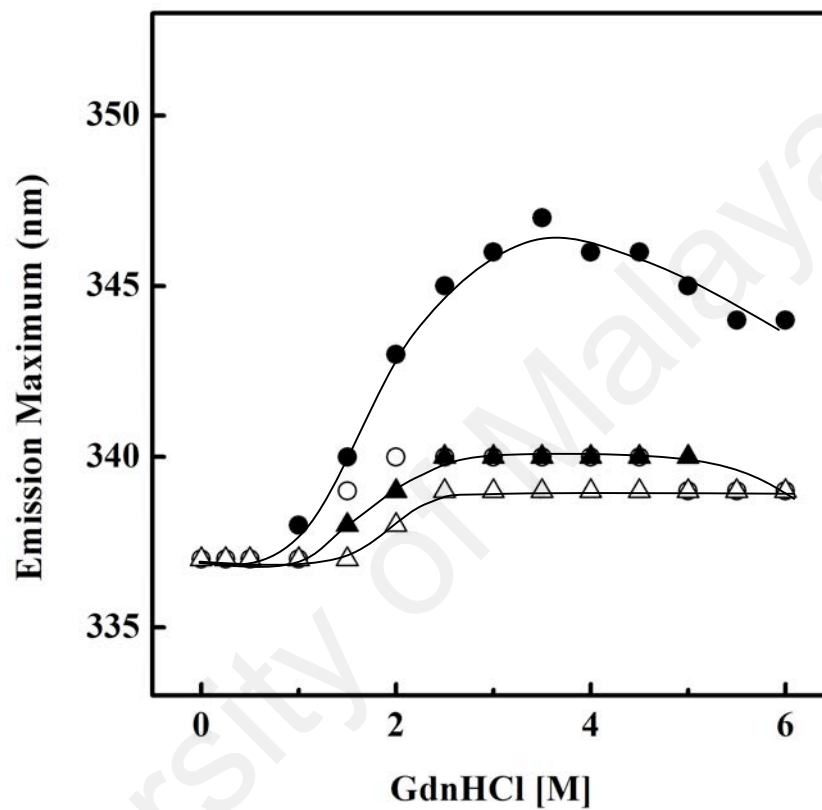
Figure 4.5   GdnHCl denaturation of native BLA in different buffers using emission maximum measurements upon excitation at 280 nm. Different buffers used were: 0.05 M sodium phosphate (●); 0.15 M Tris-HCl (○); 0.15 M HEPES (▲) and 0.15 M MOPS (△), of similar ionic strength (0.15) and pH (7.5).

fluorophores in the unfolded state due to which the spectral signal did not show any major change.

4.1.3 Ultraviolet difference spectroscopy

Since maximum structural changes were observed in 3 M GdnHCl-treated BLA in sodium phosphate buffer, when monitored by MRE_{222nm} and fluorescence intensity measurements, absorption spectroscopy was also employed to further investigate these structural changes. Figure 4.6 shows the UV absorption spectra of native and 3 M GdnHCl denatured BLAs. The UV absorption spectrum of native BLA was characterized by the presence of absorption maximum at 280 nm. Treatment of native BLA with 3 M GdnHCl showed significant decrease in the absorbance (hypochromism) and 2 nm blue shift in the emission maximum (Figure 4.6). Such difference in the absorption characteristic can be clearly seen from the UV difference spectra.

Figure 4.7 shows the UV difference spectra of 3 M GdnHCl-denatured BLA, obtained in different buffers. The difference spectra were characterized by the presence of negative spectral signals at 280 nm, 286 nm and 291 nm. Presence of these signals in the difference spectra was suggestive of the environmental perturbation of Tyr and Trp residues (Sogami and Ogura, 1973). Specifically, appearance of negative spectral signals at 280 nm and 286 nm indicated microenvironmental changes around Tyr residues of BLA, whereas presence of a negative spectral signal at 291 nm characterized microenvironmental changes around Trp residues. A comparison of these spectra showed that stronger spectral signals were obtained in sodium phosphate and Tris-HCl buffers, being highest in sodium phosphate buffer. On the other hand, HEPES and MOPS buffers showed weaker signals. Effectiveness of these buffers to produce GdnHCl-induced changes in BLA followed the same order as observed with MRE_{222nm}
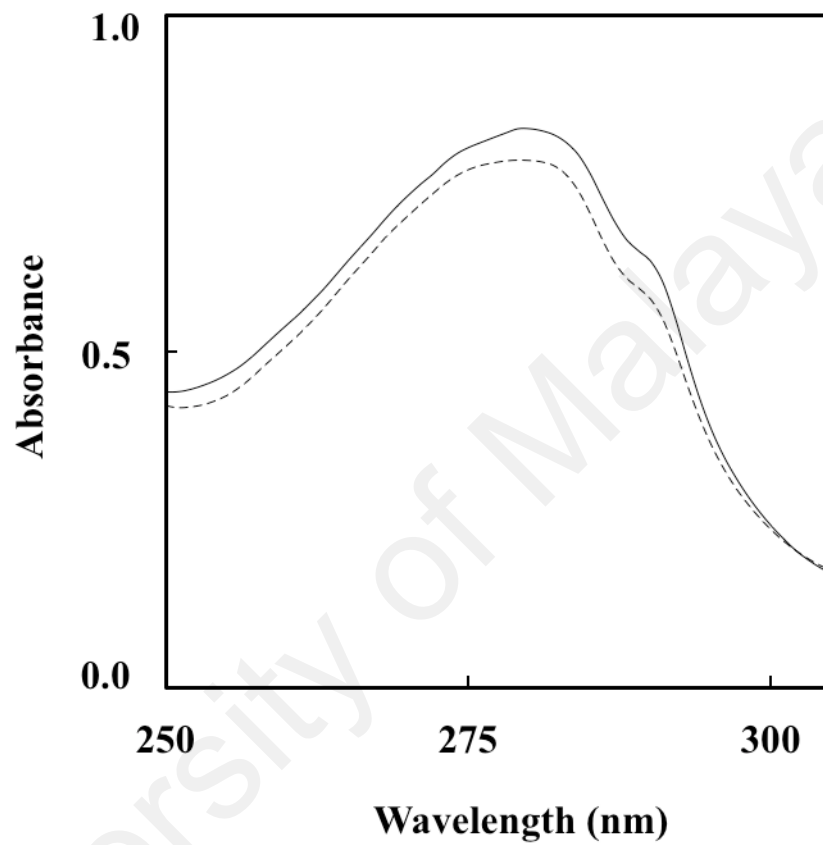
Figure 4.6 UV-absorption spectra of native BLA (solid line) and 3 M GdnHCl-denatured BLA (dotted line), as obtained in 0.05 M sodium phosphate buffer, pH 7.5.
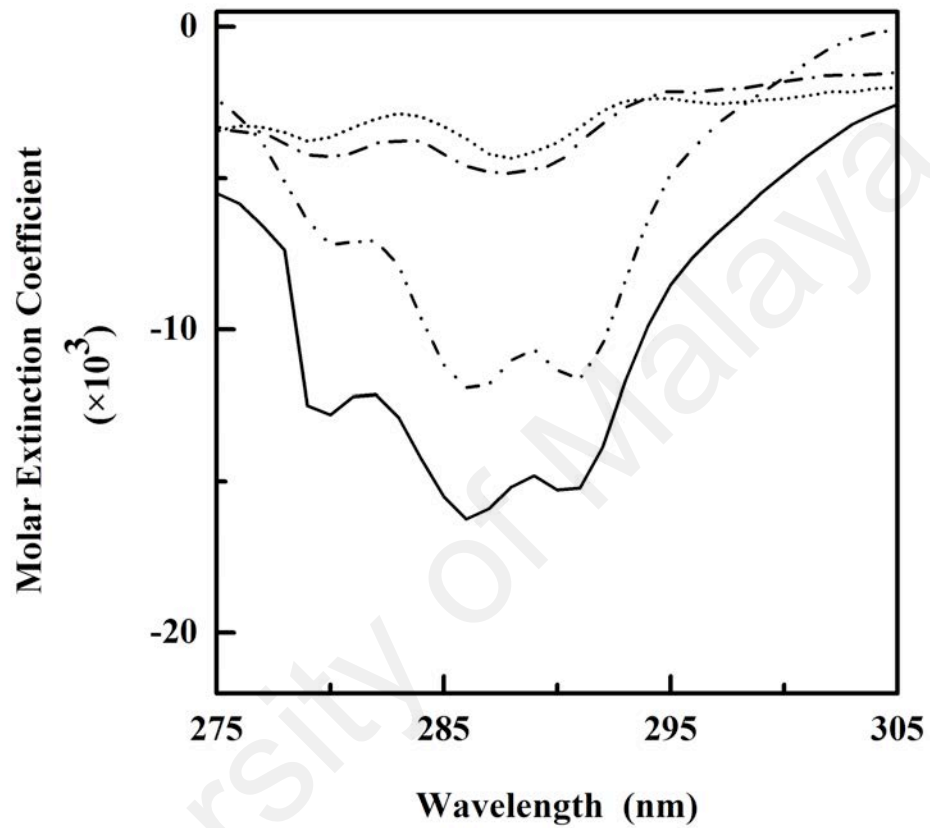
Figure 4.7   UV-difference spectra of 3 M GdnHCl-denatured BLA in different buffers. The buffers used were: 0.05 M sodium phosphate (solid line); 0.15 M Tris-HCl (dash double dot dashed line); 0.15 M HEPES (dash dot dashed line) and 0.15 M MOPS (dotted line) of similar ionic strength (0.15) and pH (7.5).

(Figure 4.2) and fluorescence measurements (Figures 4.4 and 4.5).

4.2 Effect of buffer composition on GdnHCl-induced aggregation of BLA

The possibility of GdnHCl-induced aggregation occurring at higher (> 3.5 M) GdnHCl concentrations, if any, was evaluated by gel chromatography of different BLA samples on Sephacryl S-200 HR column (1.0×30 cm). Figures 4.8–4.10 show the elution profiles of the native BLA, 3 M GdnHCl-denatured BLA and 6 M GdnHCl-denatured BLA, respectively on the same column, equilibrated with 0.05 M sodium phosphate buffer, pH 7.5 containing respective concentrations of GdnHCl. Elution profiles of blue dextran on the same column under similar experimental conditions are also included in these figures. The elution characteristics of these samples are given in Table 4.1. As can be seen from Figure 4.8, the native BLA eluted as a single symmetrical peak with an elution volume, V_e of 17.43 mL, which corresponded to a V_e/V_o value of 1.83 (Table 4.1).

The elution profile, obtained with 3 M GdnHCl-denatured BLA (Figure 4.9), also displayed a major peak, which eluted earlier than the native BLA and had an elution volume of 13.12 mL. It corresponded to a V_e/V_o ratio of 1.36. (Table 4.1). This suggested expansion in the hydrodynamic volume of the protein due to GdnHCl-induced denaturation (Roseman et al., 1975, Pace et al., 1989). In addition to the major peak, a small concentration of BLA showed retarded elution with an approximate elution volume of 16.81 mL (Table 4.1), as represented by a small broader peak in Figure 4.9. Such retardation of a few GdnHCl-denatured BLA molecules seems possible due to its interaction with the gel particles (Kruger et al., 1987, Tan et al., 2011). Interestingly, elution of 6 M GdnHCl-denatured BLA (Figure 4.10) produced a major peak with the elution volume of 9.58 mL (Table 4.1). It eluted with the void volume

Figure 4.8 Gel chromatographic profile of native BLA (1.25 mg/500 μL) on Sephacryl S-200 HR column (1.0×30 cm), equilibrated with 0.05 M sodium phosphate buffer, pH 7.5. Peak shown by the dotted line represents the elution profile of the blue dextran (2 mg/ 500 μL) on the same column.

Figure 4.9 Gel chromatographic profile of 3 M GdnHCl-denatured BLA (1.50 mg/500 μL) on Sephacryl S-200 HR column (1.0×30 cm), equilibrated with 0.05 M sodium phosphate buffer, pH 7.5 containing 3 M GdnHCl. Peak shown by the dotted line represents the elution profile of the blue dextran (2 mg/ 500 μL) on the same column.

Figure 4.10 Gel chromatographic profile of 6 M GdnHCl-denatured BLA (1.50 mg/500 µL) on Sephacryl S-200 HR column (1.0×30 cm), equilibrated with 0.05 M sodium phosphate buffer, pH 7.5 containing 6 M GdnHCl. Peak shown by the dotted line represents the elution profile of the blue dextran (2 mg/ 500 µL) on the same column.

Table 4.1 Gel chromatographic data of native and GdnHCl-denatured BLAs on Sephacryl S-200 HR column (1.0×30 cm), equilibrated with 0.05 M sodium phosphate buffer, pH 7.5 under different experimental conditions.

Protein Sample	Peak No.	V_e (mL)	V_e/V_0
Native BLA	1	17.43	1.83
3 M GdnHCl-denatured BLA	1	13.12	1.36
	2	16.81	1.74
6 M GdnHCl-denatured BLA	1	9.58	1.02
	2	11.93	1.27
	3	19.24	2.01

(9.4 mL) of the column, as V_e/V_o value for this peak was found to be 1.02 (Table 4.1). These BLA molecules falling under peak 1 may represent BLA aggregates, as peak 2 (Figure 4.10) with a V_e/V_o value of 1.27 (Table 4.1) might be referred to as GdnHCl-denatured BLA. This seems understandable, as elution volume of peak 2 (11.93 mL) was found to be lower than the elution volume of peak 1 (13.12 mL) of 3 M GdnHCl-denatured BLA, which represented the denatured form of BLA. A small change in V_e (Table 4.1) from 13.12 mL (for 3 M GdnHCl-denatured BLA) to 11.93 mL (for 6 M GdnHCl-denatured BLA) seems reasonable, as 6 M GdnHCl might have denatured the BLA completely compared to 3 M GdnHCl-denatured BLA. 6 M GdnHCl would have completely removed non-covalent interactions, compared to 3 M GdnHCl and thus had produced greater expansion in the hydrodynamic volume of the protein, which was responsible for its lower elution volume. In addition, a small fraction of the protein was also eluted as peak 3 in the elution profile (Figure 4.10), with an elution volume of 19.24 mL (Table 4.1) due to protein interaction with the gel matrix. These results clearly indicated BLA aggregation in the presence of 6 M GdnHCl.

Since different buffers *i.e* sodium phosphate, Tris-HCl, HEPES and MOPS buffers produced differential effects upon GdnHCl denaturation of BLA as revealed by the spectral signals (MRE_{222nm} and fluorescence intensity at 337 nm) shown in Figures 4.2 and 4.4, it was interesting to investigate the effect of these buffers on GdnHCl-induced aggregation of BLA. Figures 4.11–4.13 show the elution behavior of native BLA, 3 M GdnHCl-denatured BLA and 6 M GdnHCl-denatured BLA on the Sephacryl S-200 HR column, equilibrated with 0.15 M Tris-HCl buffer, pH 7.5 under similar conditions with respect to GdnHCl concentration. Similar to the results obtained in 0.05 M sodium phosphate buffer, pH 7.5 (Figure 4.8), a single symmetrical peak
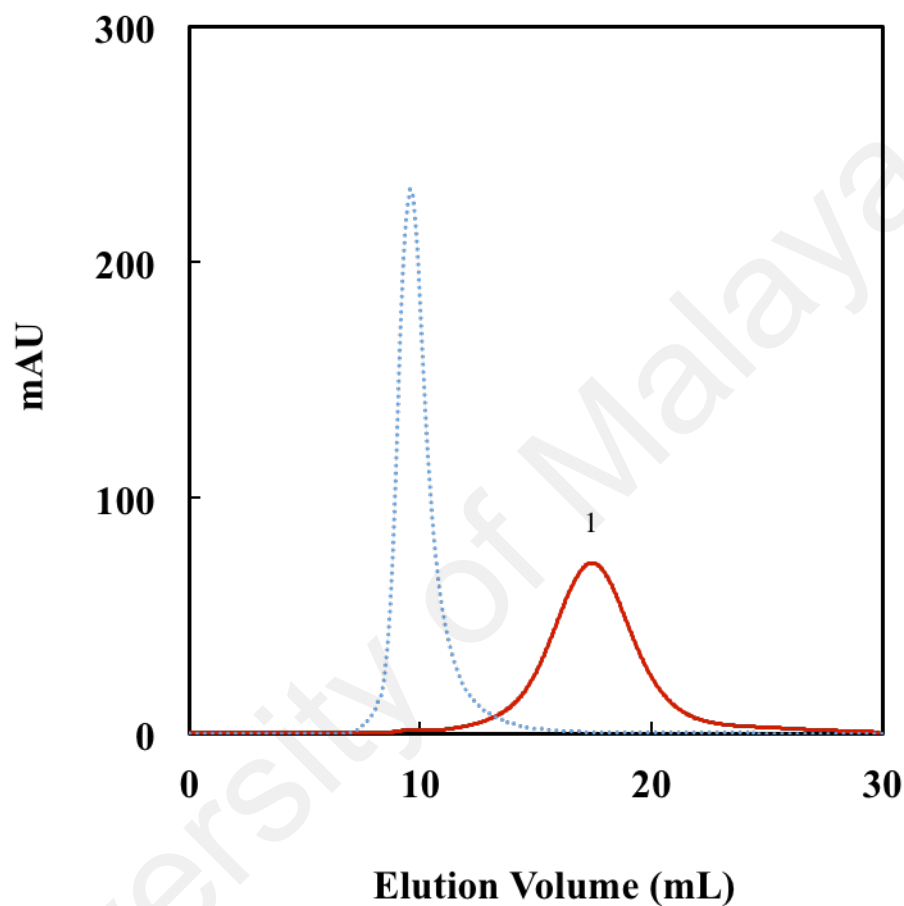
Figure 4.11 Gel chromatographic profile of native BLA (1.25 mg/500 µL) on Sephacryl S-200 HR column (1.0×30 cm), equilibrated with 0.15 M Tris-HCl buffer, pH 7.5. Peak shown by the dotted line represents the elution profile of the blue dextran (2 mg/ 500 µL) on the same column.
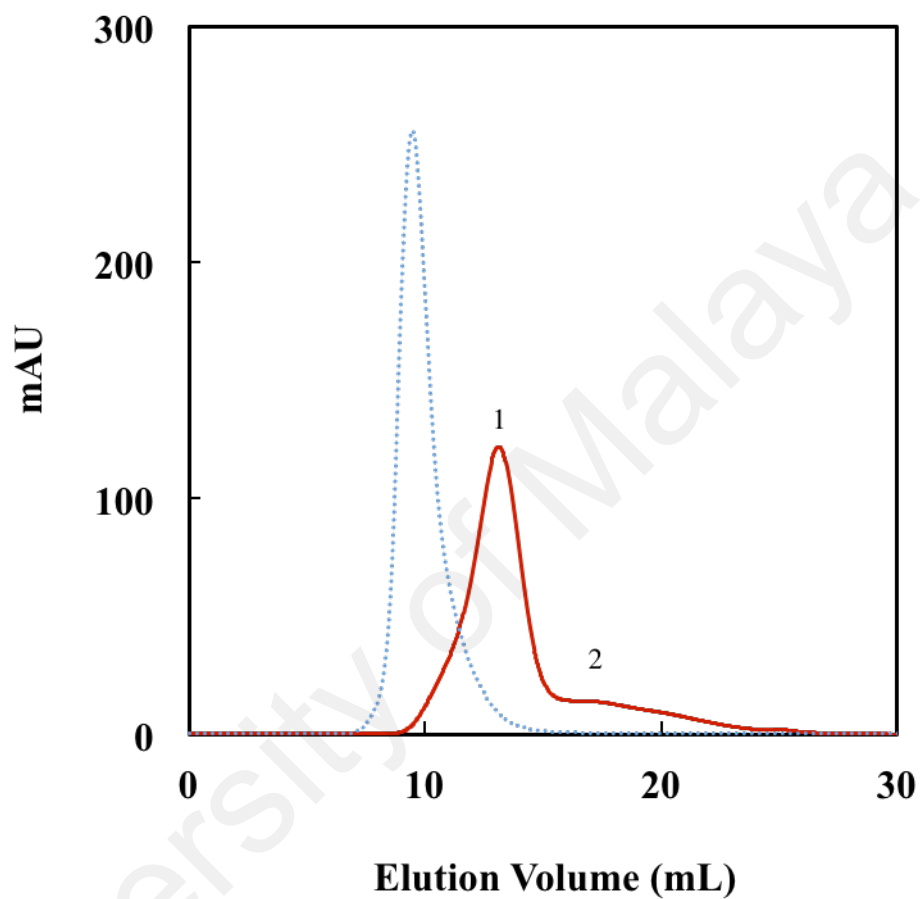
Figure 4.12 Gel chromatographic profile of 3 M GdnHCl-denatured BLA (1.25 mg/500 μL) on Sephacryl S-200 HR column (1.0×30 cm), equilibrated with 0.05 M Tris-HCl buffer, pH 7.5 containing 3 M GdnHCl. Peak shown by the dotted line represents the elution profile of the blue dextran (2 mg/ 500 μL) on the same column.
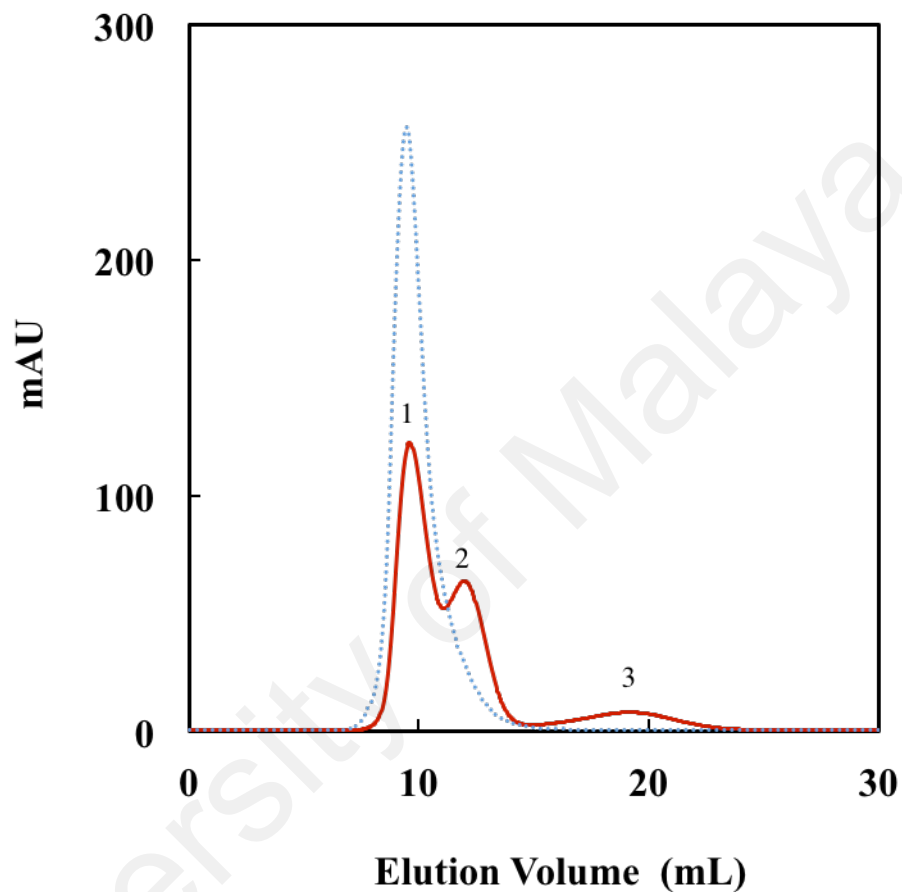
Figure 4.13 Gel chromatographic profile of 6 M GdnHCl-denatured BLA (1.50 mg/500 µL) on Sephacryl S-200 HR column (1.0×30 cm), equilibrated with 0.15 M Tris-HCl buffer, pH 7.5 containing 6 M GdnHCl. Peak shown by the dotted line represents the elution profile of the blue dextran (2 mg/ 500 µL) on the same column.

Table 4.2 Gel chromatographic results of native and GdnHCl-denatured BLAs on Sephacryl S-200 HR column (1.0×30 cm), equilibrated with 0.15 M Tris-HCl buffer, pH 7.5 under different experimental conditions.

Protein Sample	Peak No.	V_e (mL)	V_e/V_0
Native BLA	1	15.75	1.64
3 M GdnHCl-denatured BLA	1	13.12	1.36
	2	15.71	1.74
6 M GdnHCl-denatured BLA	1	9.62	1.03
	2	11.96	1.28
	3	19.24	2.06

(Figure 4.11) with an elution volume of 15.75 mL and the corresponding V_e/V_0 value of 1.64 (Table 4.2) was observed with native BLA. Smaller changes in the V_e/V_0 value of native BLA, obtained in two different buffers were not common and had been reported earlier (Aimar and Meireles, 2010). This can be clearly seen from the elution patterns (Figures 4.12 and 4.13) and elution characteristics (Table 4.2) of 3 M and 6 M GdnHCl-denatured BLAs, obtained in 0.15 M Tris-HCl buffer, pH 7.5, which were found similar within experimental error, to those obtained in 0.05 M sodium phosphate buffer, pH 7.5 (Figures 4.9 and 4.10, Table 4.1).

Interestingly, when gel chromatographic analyses of native, 3 M GdnHCl-denatured and 6 M GdnHCl-denatured BLAs were made on the same Sephacryl S-200 HR column, equilibrated with either 0.15 M HEPES buffer, pH 7.5 (Figures 4.14−4.16, Table 4.3) or 0.15 M MOPS buffer, pH 7.5 (Figures 4.17−4.19, Table 4.4), no significant variation in the V_e/V_o values of the major peaks was observed. Furthermore, these V_e/V_o values were similar to those obtained with sodium phosphate or Tris-HCl buffers (Tables 4.1−4.4). These results clearly suggested formation of similar denatured states and aggregated forms of BLA in 3 M and 6 M GdnHCl in the presence of these buffers. However, quantitative differences in BLA aggregation were noticed in these buffers in the presence of 6 M GdnHCl, as revealed by the differences in the peak areas under peak 1 and peak 2 (Figures 4.10, 4.13, 4.16 and 4.19). Due to the lack of the software, peak areas under these peaks could not be evaluated.

These results, clearly demonstrated that differences observed in the spectral signals upon GdnHCl treatment of BLA in the presence of these buffers can not be ascribed to the stabilization of BLA with HEPES and MOPS buffers against GdnHCl denaturation.

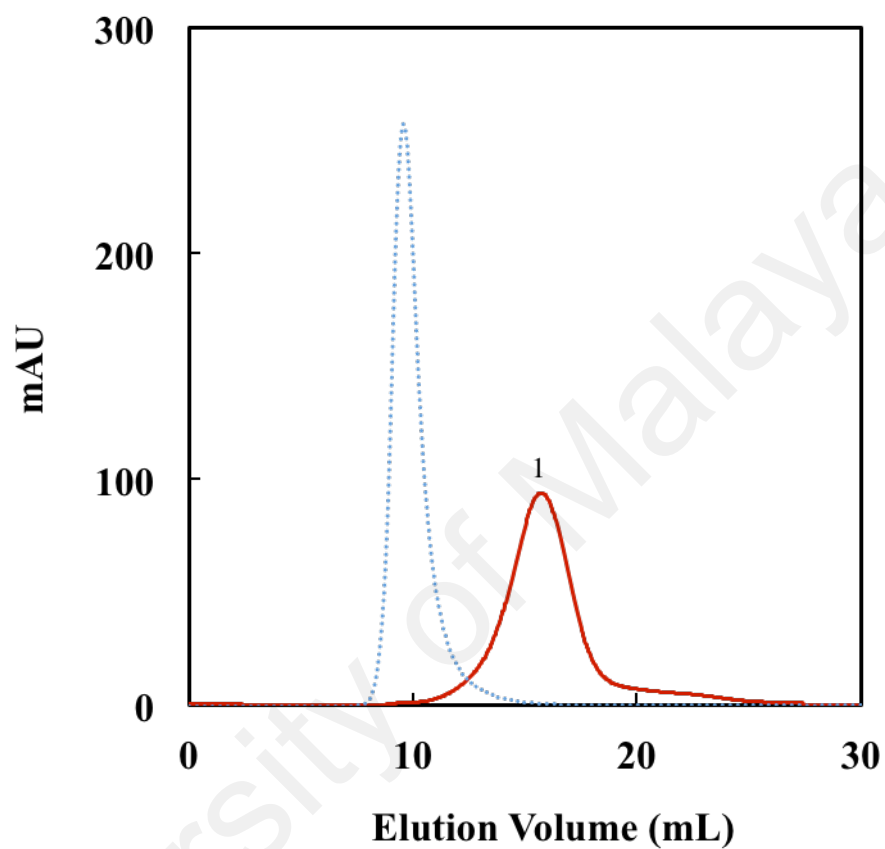**Figure 4.14** Gel chromatographic profile of native BLA (1.25 mg/500 µL) on Sephacryl S-200 HR column (1.0×30 cm), equilibrated with 0.15 M HEPES buffer, pH 7.5. Peak shown by the dotted line represents the elution profile of the blue dextran (2 mg/ 500 µL) on the same column.
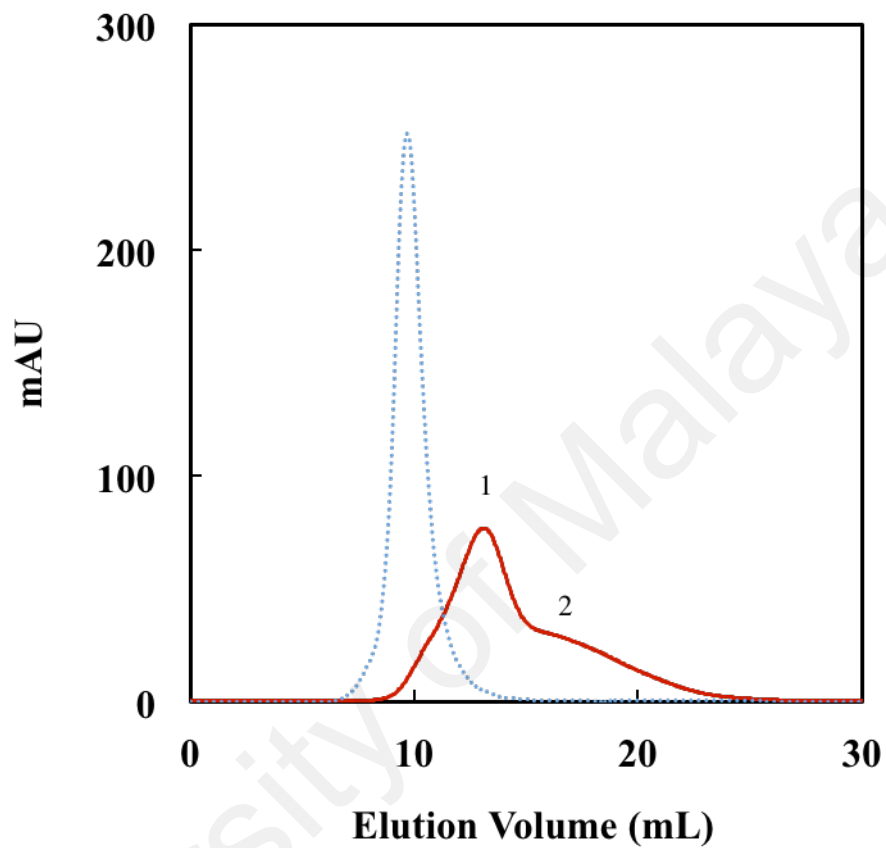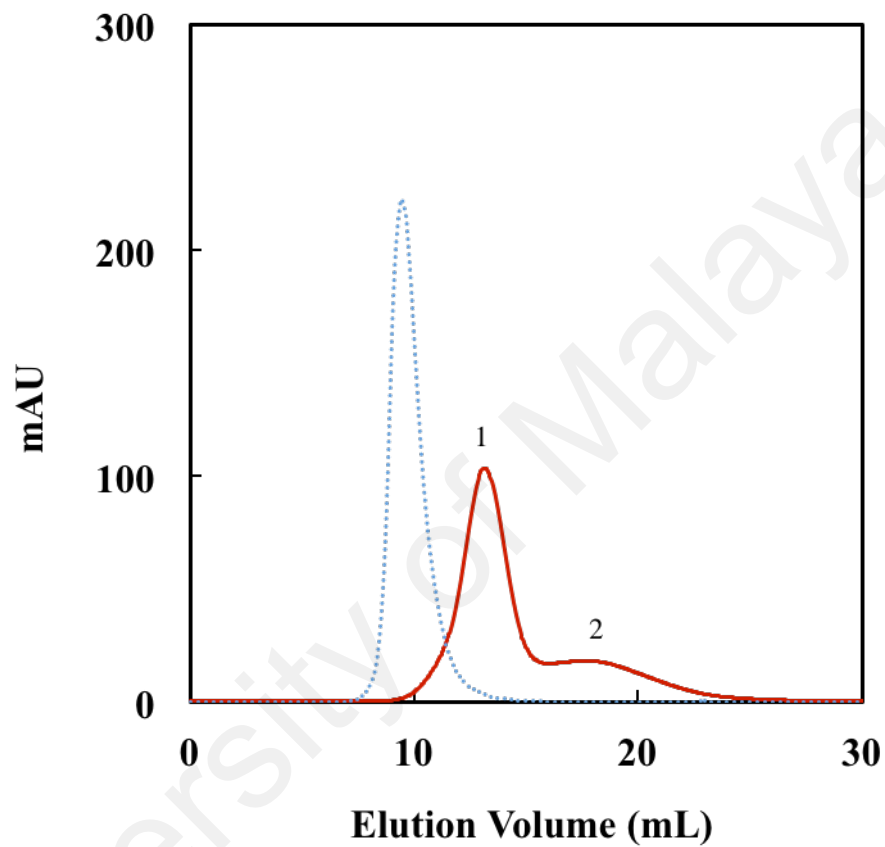
Figure 4.15 Gel chromatographic profile of 3 M GdnHCl-denatured BLA (1.50 mg/500 μL) on Sephacryl S-200 HR column (1.0×30 cm), equilibrated with 0.15 M HEPES buffer, pH 7.5 containing 3 M GdnHCl. Peak shown by the dotted line represents the elution profile of the blue dextran (2 mg/ 500 μL) on the same column.
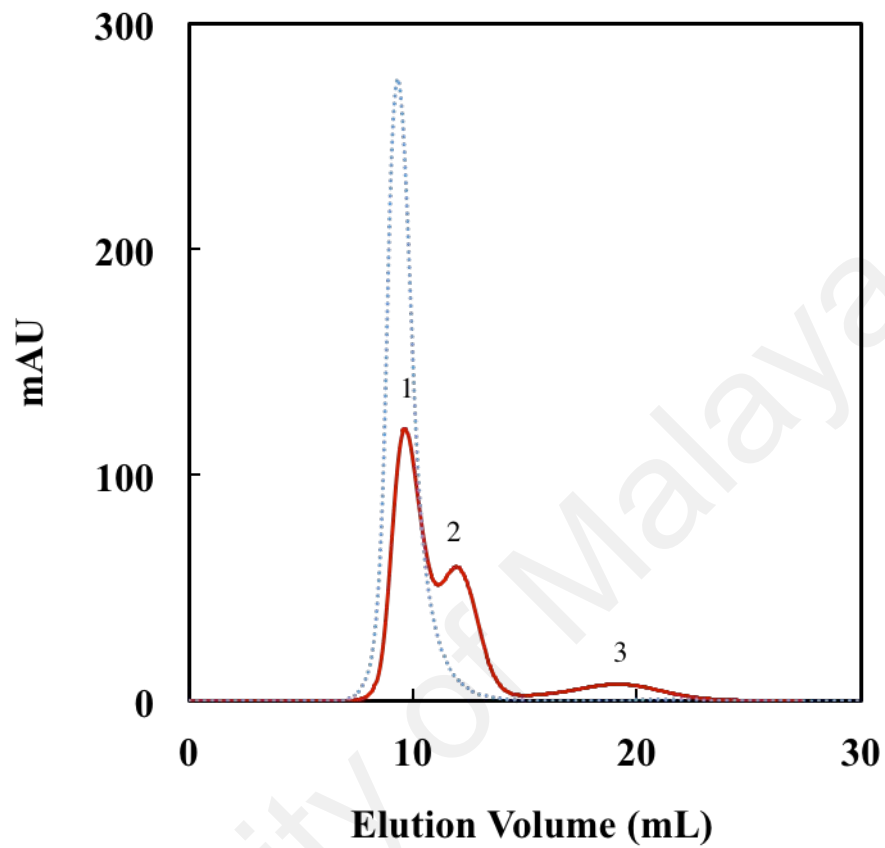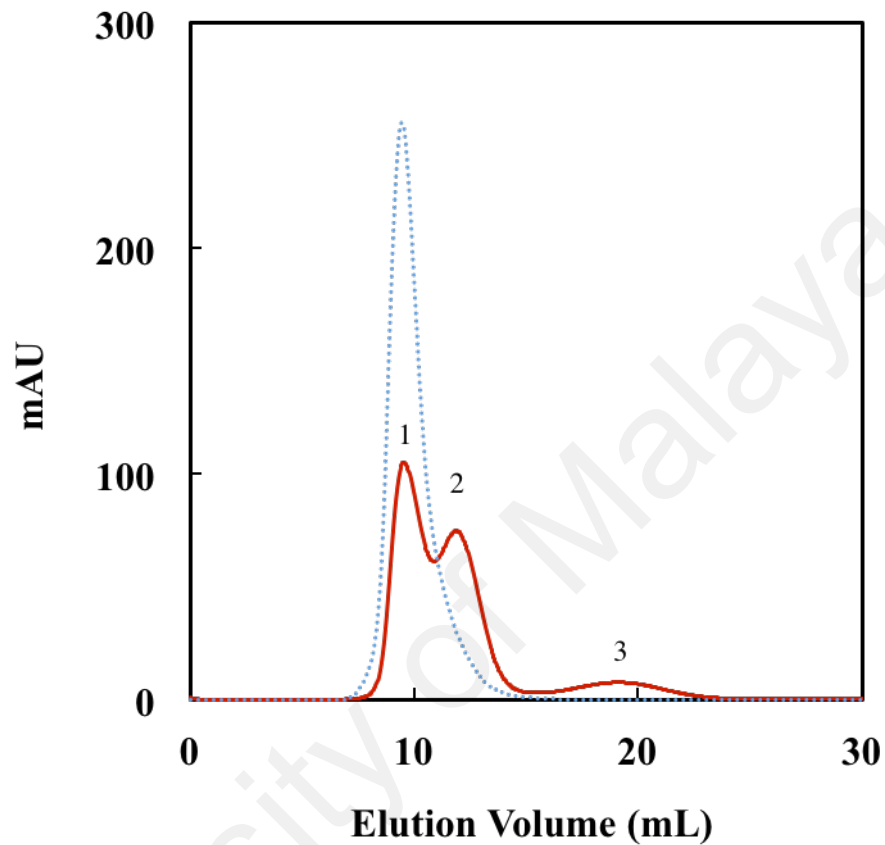
Figure 4.16 Gel chromatographic profile of 6 M GdnHCl-denatured BLA (1.50 mg/500 µL) on Sephacryl S-200 HR column (1.0×30 cm), equilibrated with 0.15 M HEPES buffer, pH 7.5 containing 6 M GdnHCl. Peak shown by the dotted line represents the elution profile of the blue dextran (2 mg/ 500 µL), on the same column.

Table 4.3 Gel chromatographic results of data and GdnHCl-denatured BLAs on Sephacryl S-200 HR column (1.0×30 cm), equilibrated with 0.15 M HEPES buffer, pH 7.5 under different experimental conditions.

Protein Sample	Peak No.	V_e (mL)	V_e/V_0
Native BLA	1	16.36	1.70
3 M GdnHCl-denatured BLA	1	13.18	1.39
	2	14.71	1.64
6 M GdnHCl-denatured BLA	1	9.51	1.00
	2	11.86	1.25
	3	19.04	2.01
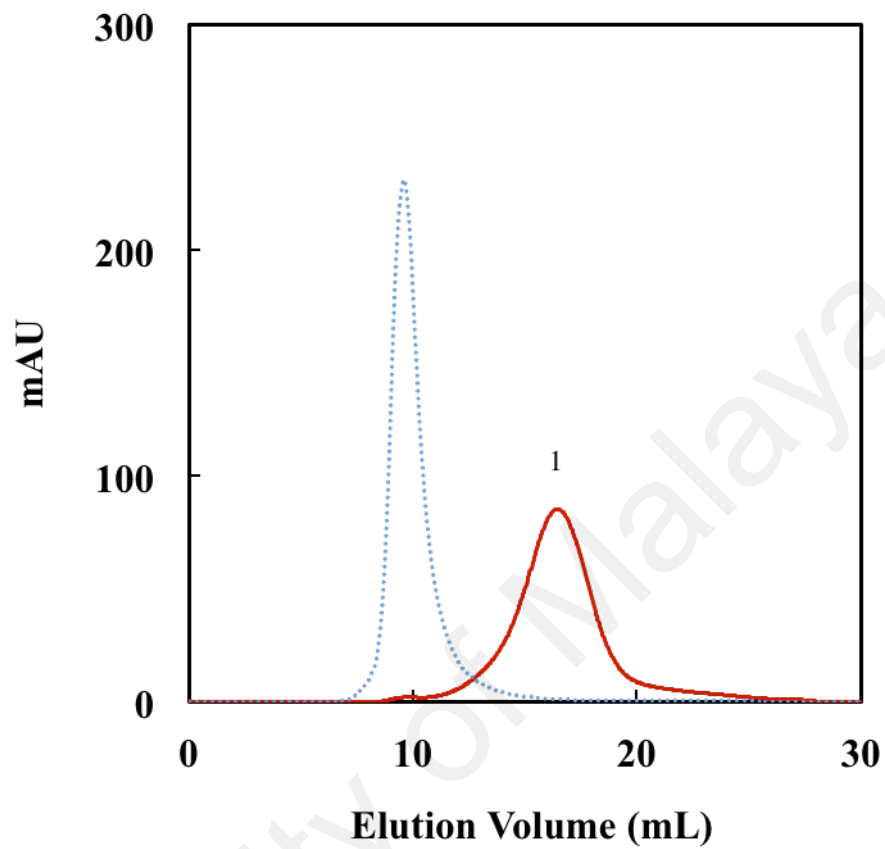
Figure 4.17   Gel chromatographic profile of native BLA (1.25 mg/500 µL) on Sephacryl S-200 HR column (1.0×30 cm), equilibrated with 0.15 M MOPS buffer, pH 7.5. Peak shown by the dotted line represents the elution profile of the blue dextran (2 mg/ 500 µL) on the same column.
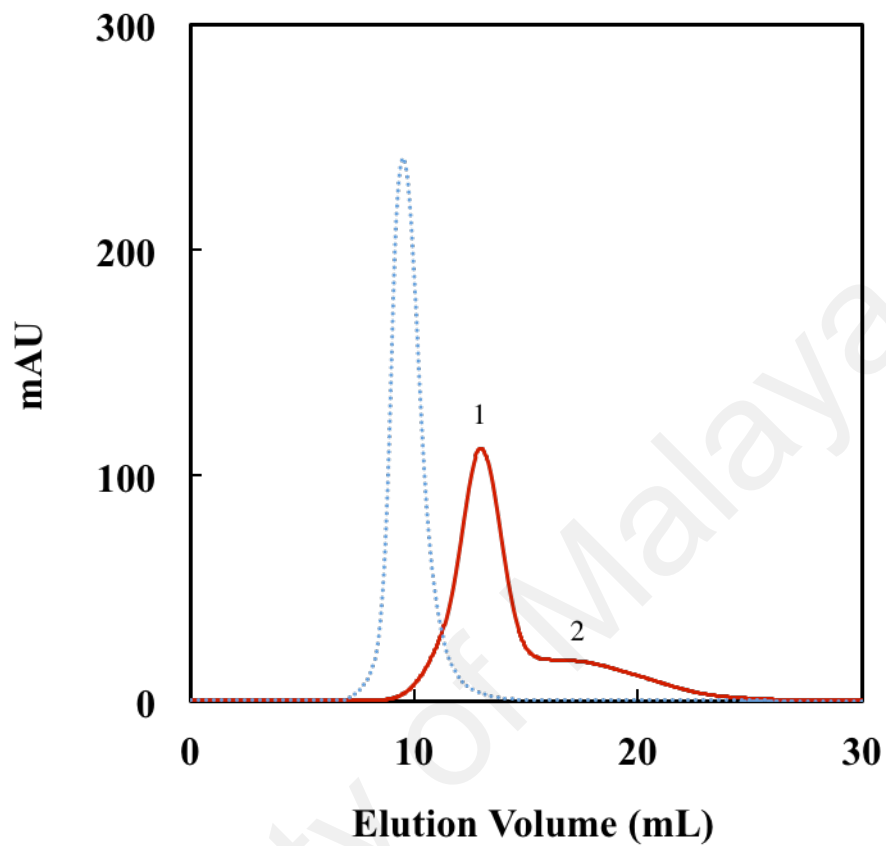
Figure 4.18 Gel chromatographic profile of 3 M GdnHCl-denatured BLA (1.50 mg/500 µL) on Sephacryl S-200 HR column (1.0×30 cm), equilibrated with 0.15 M MOPS buffer, pH 7.5 containing 3 M GdnHCl. Peak shown by the dotted line represents the elution profile of the blue dextran (2 mg/ 500 µL) on the same column.
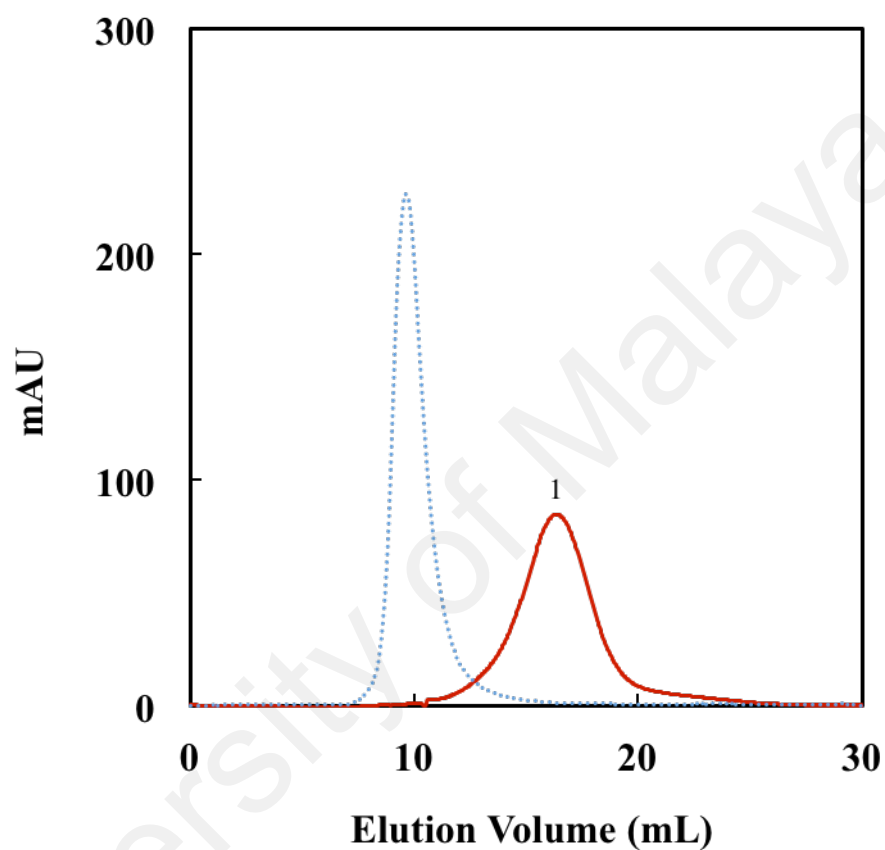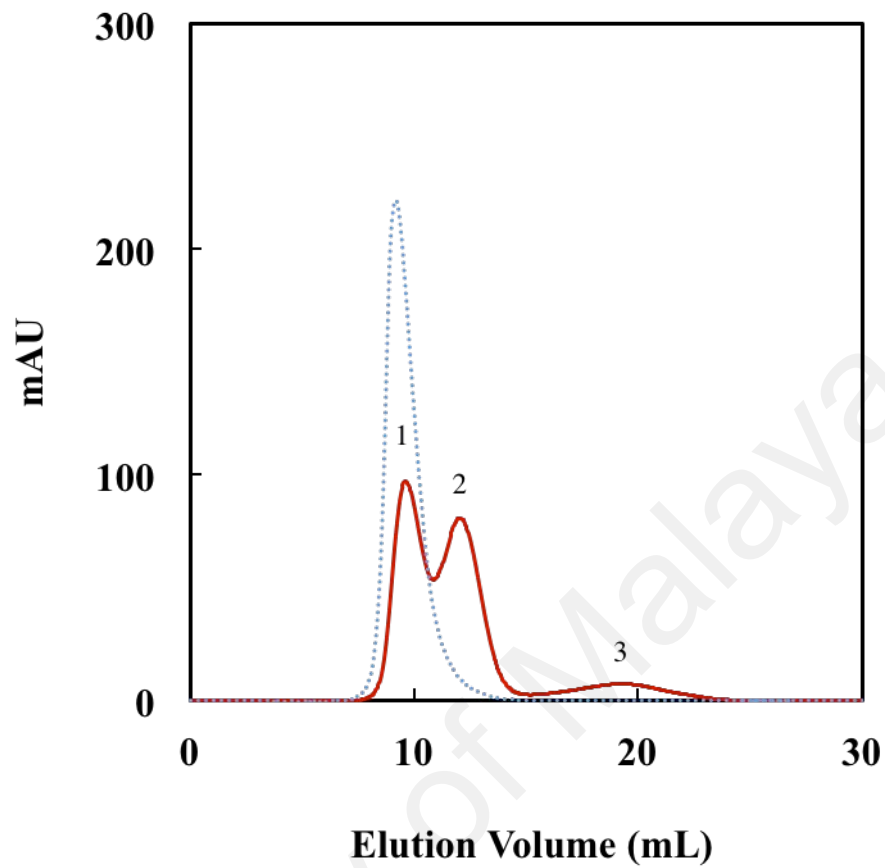
Figure 4.19 Gel chromatographic profile of 6 M GdnHCl-denatured BLA (1.50 mg/500 µL) on Sephacryl S-200 HR column (1.0×30 cm), equilibrated with 0.15 M MOPS buffer, pH 7.5 containing 6 M GdnHCl. Peak shown by the dotted line represents the elution profile of the blue dextran (2 mg/ 500 µL) on the same column.

Table 4.4 Gel chromatographic results of data and GdnHCl-denatured BLAs on Sephacryl S-200 HR column (1.0×30 cm), equilibrated with 0.15 M MOPS buffer, pH 7.5 under different experimental conditions.

Protein Sample	Peak No.	V_e (mL)	V_e/V_0
Native BLA	1	16.52	1.72
3 M GdnHCI-denatured BLA	1	13.00	1.37
	2	15.71	1.74
6 M GdnHCI-denatured BLA	1	9.61	1.00
	2	12.00	1.30
	3	19.20	2.09

4.3 Effect of buffer composition on GdnHCl denaturation of Ca-depleted BLA

As calcium is known to offer stability to BLA (Declerck et al., 2002), we also checked the effect of buffer composition on GdnHCl denaturation of Ca-depleted BLA. In the absence of calcium, differential effects observed with different buffers on GdnHCl denaturation of BLA (Figures 4.2 and 4.4) should have been maximized. Figure 3.19 shows the effect of different buffer composition on GdnHCl denaturation of Ca-depleted BLA, when examined by fluorescence intensity measurements at 337 nm (Figure 4.20) and emission maximum (Figure 4.21). GdnHCl treatment produced a decrease in the fluorescence intensity up to 1.0 M GdnHCl concentration, which remained unchanged or showed slight variation up to 6.0 M GdnHCl. The decrease was drastic in both sodium phosphate and Tris-HCl buffers, but mild in HEPES and MOPS buffers (Figure 4.20). Quantitatively, ~ 65 % decrease in the fluorescence intensity was observed in sodium phosphate buffer against 48 % decrease, obtained in Tris-HCl buffer at 1.0 M GdnHCl. On the other hand, HEPES and MOPS buffers produced ~34 % and ~28 % decrease in the fluorescence intensity, respectively, at 1.0 M GdnHCl. The magnitude of the decrease in the fluorescence intensity observed in these buffers with Ca-depleted BLA was much higher than that obtained with native BLA (Figure 4.4). Presence of calcium in the native BLA might be responsible for such difference.

In addition to the decrease in the fluorescence intensity, GdnHCl also produced shift in the emission maximum. Figure 4.21 shows changes in the emission maximum with increasing GdnHCl concentrations in different buffers. Sodium phosphate buffer produced the maximum change, showing 12 nm red shift (from 337 nm to 349 nm, characteristic of solvent-exposed Trp residues) at 2.5 M GdnHCl concentration, which leveled off thereafter reaching 341 nm at 6 M GdnHCl due to protein aggregation. These results were qualitatively similar to those shown in Figure 4.5. However, a more
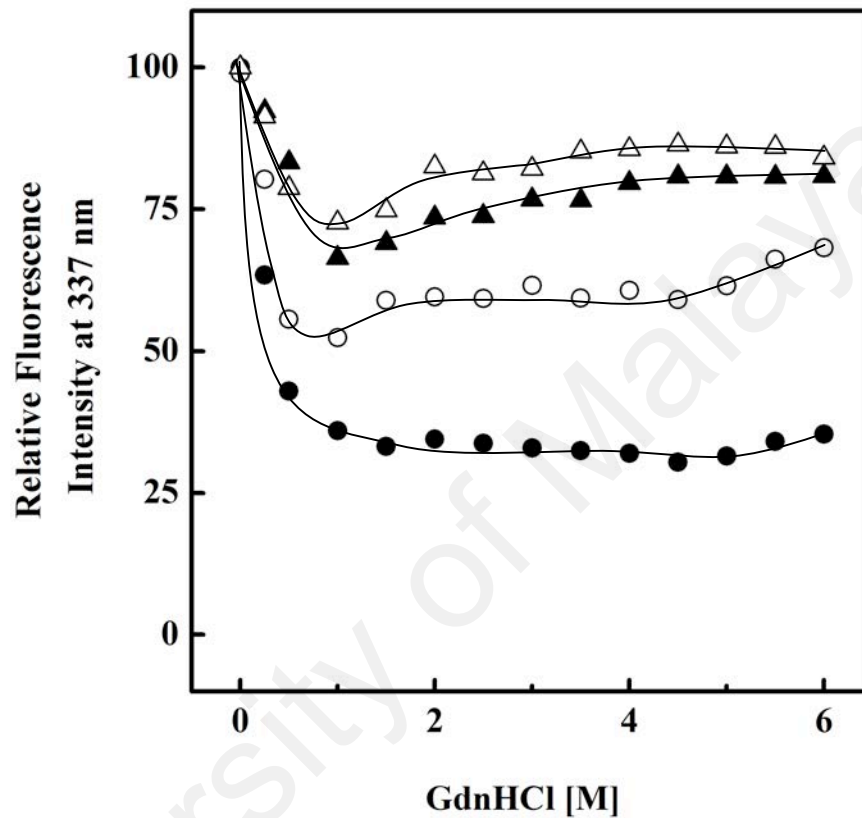
Figure 4.20 GdnHCl denaturation of calcium-depleted BLA in different buffers using intrinsic fluorescence measurements at 337 nm upon excitation at 280 nm. Different buffers used were: 0.05 M sodium phosphate (●); 0.15 M Tris-HCl (○); 0.15 M HEPES (▲) and 0.15 M MOPS (△), of similar ionic strength (0.15) and pH (7.5).
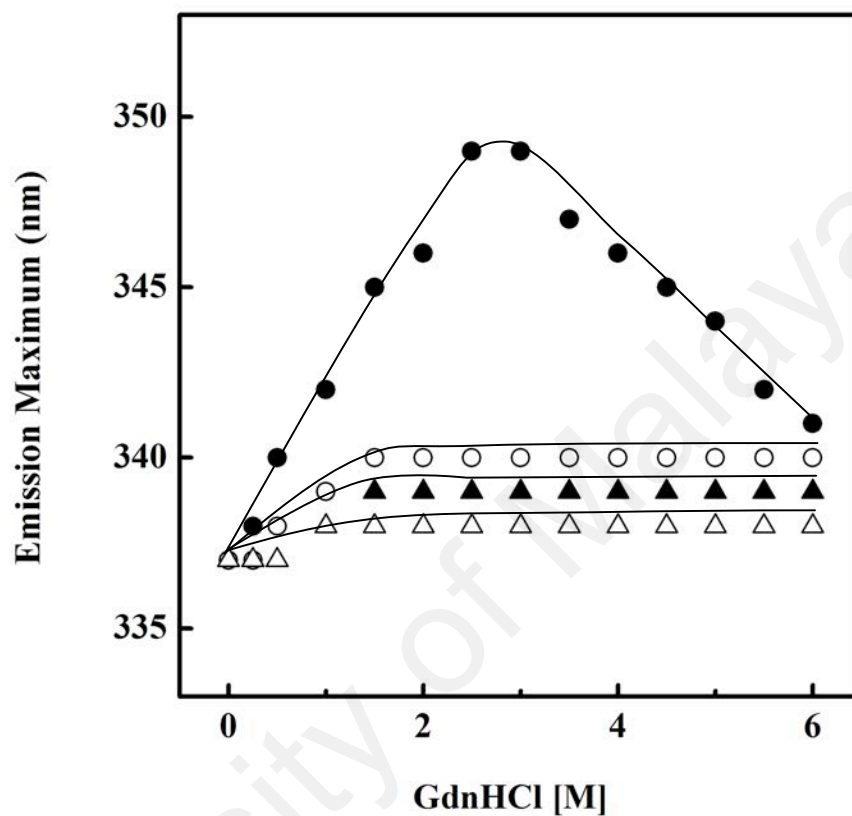
Figure 4.21 GdnHCl denaturation of calcium-depleted BLA in different buffers using emission maximum measurements upon excitation at 280 nm. Different buffers used were: 0.05 M sodium phosphate (●); 0.15 M Tris-HCl (○); 0.15 M HEPES (▲) and 0.15 M MOPS (△), of similar ionic strength (0.15) and pH (7.5).

pronounced red shift at 2.5 M GdnHCl was observed with Ca-depleted BLA, compared to native BLA, which can be ascribed to the presence of calcium in the native BLA. On the other hand, about 1-3 nm red shift was observed with MOPS, HEPES and Tris-HCl buffers at 1.5 M GdnHCl, which remained unchanged up to 6 M GdnHCl.

Both the decrease in the fluorescence intensity and red shift in the emission maximum are usually taken as indicators of protein denaturation (Duy et al., 2006). A comparison of the results obtained with native BLA (Figure 3.4 and 3.5) and Ca-depleted BLA (Figures 4.20 and 4.21) suggested a greater extent of denaturation of Ca-depleted BLA, compared to native BLA at any GdnHCl concentration. This seems understandable as native BLA contained some bound calcium to it, which is known to provide structural stability (Declerck et al., 2002). Furthermore, the differential effects of buffer composition were found to be similar with Ca-depleted BLA to that obtained with native BLA, showing the effectiveness of these buffers in the order: sodium phosphate > Tris-HCl > HEPES > MOPS. Whether lesser extents of spectral changes, observed with HEPES and MOPS buffers in the presence of GdnHCl were due to some other factors need to be further investigated.

CONCLUSION

5. CONCLUSION

Taken together, the results suggested the influence of buffer composition on GdnHCl denaturation of BLA. Whereas, maximum change in the spectral signal was observed with sodium phosphate buffer followed by Tris-HCl buffer, both HEPES and MOPS buffers showed lesser spectral changes. The stabilizing effect of calcium was evident from the greater extent of spectral change, observed with Ca-depleted BLA compared to native BLA. Although CD and fluorescence spectral signals showed the differential effects of buffers, gel chromatography of 3 M - and 6 M GdnHCl-denatured BLAs demonstrated the formation of similar denatured states and aggregated forms in these buffers.

REFERENCES

6. REFERENCES

Ahmad, B., Ahmed, M.Z., Haq,. S.K. and Khan, R.H. (2005). Guanidine hydrochloride denaturation of human serum albumin originates by local unfolding of some stable loops in domain III. *Biochimica et Biophysica Acta, 1750*: 93 –102.

Aimar, P. and Meireles, M. (2010). Calibration of ultrafiltration membranes against size exclusion chromatography colums. *Journal of Membrane Science, 364*: 233 – 239.

Alonso, D.O. and Dill K.A. (1991). Solvent denaturation and stabilization of globular proteins. *Biochemistry*, *30*: 5974 –5985.

Ammar, Y.B., Matsubara, T., Ito, K., Iizuka, M., Limpaseni, T., Pongsawasdi, P. and Minamiura, N. (2002). New action pattern of a maltose-forming α-amylases from *Streptomyces sp*. and its possible application in bakery. *Journal of Biochemistry and Molecular Biology, 35*: 568 –575.

Anfinsen, C.B. (1973). Principles that govern the folding of protein chains. *Science*, *181*: 223 –230.

Arasaratnam, V. and Balasubramaniam, K. (1992). Synergistic action of alpha amylase and glucoamylase on raw starch. *Journal of Microbial Biotechnology, 7:* 37 –46.

Arnold, F.H., Wintrode, P.L., Miyazaki, K. and Gershenson, A. (2001). How enzymes adapt: Lessons from directed evolution. *Trends in Biochemical Sciences*, *26*: 100 –106.

Asghari, S.M., Khajeh, K., Moradian, F., Ranjbar, B. and Naderi-Manesh, H. (2004).

Acid-induced conformational changes in *Bacillus amyloliquefaciens* α-amylases: Appearances of a molten globule like state. *Enzyme and Microbial Technology, 35*: 51 –57.

Bessler, C., Schmitt, J., Maurer, K.H. and Schmid, R.D. (2003). Directed evolution of a bacterial α-amylases: Towards enhanced pH-performance and higher specific activity. *Protein Science*, *12*: 2141– 2149.

Brennan, J.D., Benjamin, D., Dibattista, E. and Gulcev, M.D. (2003). Using sugar and amino acid additives to stabilize enzymes within sol-gel derived silica. *Chemistry of Materials*, *15*, 737 –745.

Broadley, S.A. and Hartl, F.U. (2009). The role of molecular chaperones in human misfolding diseases. *FEBS Letters, 583*: 2647 –2653.

Callis, P.R. (1997). ^1L_a and ^1L_b transitions of tryptophan: Applications of theory and experimental observations to fluorescence of proteins. *Methods in Enzymology, 278*: 113 –150.

Chiang, J.P., Alter, J.E. and Elkhart, M.S. (1979). Purification and characterization of a thermostable alpha-amylase from *Bacillus licheniformis. Starch-Starke, 31*: 86 – 92.

Damodara Rao, M., Pumima, A., Ramesh, D.V. and Ayyana, C. (2002). Purification of α-amylase from *Bacillus licheniformis* by chromatofocusing and gel filtration chromatography. *World Journal of Microbiology and Biotechnology, 18*: 547 – 550.

Declerck, N., Joyet, P., Gaillardin, C.M and Masson, J.M. (1990). Use of amber

suppressors to investigate the thermostability of *Bacillus licheniformis* α-amylase. *Journal of Biological Chemistry, 265*: 15481 –15488.

Declerck, N., Joyet, P., Trosset, J.Y., Gamier, J. and Gaillardin, C.M (1995). Hyperthermostable mutants of *Bacillus licheniformis* α-amylase. Multiple amino acid replacements and molecular modelling. *Protein Engineering*, *8*: 1029 – 1037.

Declerck, N., Machius, M., Joyet, P., Wiegand, G., Huber, R. and Gaillardin, C. (2002). Engineering the thermostability of *Bacillus licheniformis* α-amylase. *Biologia Bratislava, 57*: 203 –211.

Demirkan, E.S., Mikami, B., Adachi, M., Higasa, T. and Utsumi, S. (2005). A-Amylase from *B.amyloliquefaciens*: Purification, characterization, raw starch degradation and expression in *E. coli*. *Process Biochemistry, 40*: 2629–2636.

Dill, K.A. and Shortle, D. (1991). Denatured states of proteins. *Annual Review of Biochemistry, 60:* 795 –825.

Duy, C. and Fitter, J. (2006). How aggregation and conformational scrambling of unfolded states govern fluorescence emission spectra. *Journal of Biophysics, 90*: 3704 –3711.

Egas, M.C, da Costa, M.S., Cowan, D.A. and Pires, E.M. (1988). Extracellular α-amylase from *Thermus filiformis* Ork A2: Purification and biochemical characterization. *Extremophiles*, *12*: 23 –32.

Endo, S. (1988) In: The Amylase Society of Japan (Ed.), *Handbook of Amylases and*

Related Enzymes. (pp. 47). Oxford: Pergamon Press.

Esteve- Romero, J.S., Bossi, A. and Righetti, P.G. (1996). Purification of thermamylase in multicompartment electrolyzers with isoelectric membranes: The problem of protein solubility. *Electrophoresis*, *17*: 1242 –1247.

Fágáin, C.O. (1995). Understanding and increasing protein stability. *Biochimica et Biophysica Acta*, *1252*: 1–14.

Fágáin, C.O. and O'Kennedy, R. (1991). Functionally-stabilized proteins. *Biotechnology Advances*, *9*: 351 –409.

Feller, G., d'Amico, D. and Gerday, C. (1999). Thermodynamic stability of a cold-active α-amylase from the Antartic bacterium *Alteromonas haloplanctis*. *Biochemistry, 38*: 4613 –4619.

Feller, G., Payan, F., Theys, F., Qian, M., Haser, R. and Gerday, C. (1994). Stability and structural analysis of α-amylase from the antarctic psychrophile *Alteromonas haloplanctis* A23. *European Journal of Biochemistry*, *222*: 441 – 447.

Fitter J. (2005). Structural and dynamical features contributing to the thermostability in α-amylases. *Cellular and Molecular Life Sciences*, *62*: 1925 –1937.

Fitter, J. and Haber-Pohlmeier, S. (2004). Structural stability and unfolding properties of thermostable bacterial α-amylases: A comparative study of homologous enzymes. *Biochemistry*, *43*: 9589 –9599.

Gianni, S., Ivarsson, Y., Jemth, P., Brunori M. and Travaglini-Allocatelli, C. (2007).

Identification and characterization of protein folding intermediates. *Biophysical Chemistry, 128*: 105 –113.

Griffin, S., Higgins C.L., Soulimane, T. and Wittung-Stasfshede, P. (2003). High thermal and chemical stability of *Thermus thermophilus* seven-iron ferredoxin. Linear clusters form at high pH on polypeptide unfolding. *European Journal of Biochemistry, 270*: 4736 –4743.

Haddaoui, E.A., Leloup, L., Petit-Glatron, M.F. and Chambert, R. (1997). Characterization of a stable intermediate trapped during reversible refolding of *Bacillus subtilitis* α-amylase. *European Journal of Biochemistry, 249*: 505 –509.

Halim, A.A.A., Feroz, S.R. and Tayyab, S. (2013). Does recovery in the spectral characteristics of GdnHCl-denatured *Bacillus licheniformis* α-amylase due to added calcium point towards protein stabilization? *Biophysics, Biotechnology and Biochemistry, 77*: 87 –96.

Halim, A.A.A., Kadir, H.A. and Tayyab, S. (2008). Bromophenol blue binding as a probe to study urea and guanidine hydrochloride denaturation of bovine serum albumin. *Journal of Biochemistry, 144*: 33 –38.

Hamilton, L.M., Kelly, C.T. and Fogarty, W.M. (1999a). Purification and properties of the raw starch-digesting α-amylase of *Bacillus* sp. IMD 434. *Biotechnology Letters, 21*: 111 –115.

Hamilton, L.M., Kelly, C.T. and Fogarty, W.M. (1999b). Purification and properties of the raw starch-digesting α-amylase of *Bacillus* sp. IMD 435. *Process Biochemistry, 35*: 27 –31.

Hayashida, S. and Teramoto, Y. (1986). Production and characteristics of raw-potato-starch-digesting α-amylase from Bacillus subtilis 65. *Applied and Environmental Microbiology, 54*: 1516–1522.

Hmidet, N., Bayoudh, A., Berrin, J.G., Kanoun, S., Juge, N. and Nasri, M. (2008). Purification and biochemical characterization of a novel α-amylase from *Bacillus licheniformis* NHI: Cloning, nucleotide sequence and expression of gene in *Escherichia coli. Process Biochemistry, 43*: 499 –510.

Imoto, T. (1997). Stabilization of protein. *Cellular and Molecular Life Sciences*, *53*: 215 –223.

Inagaki, K., Tanizawa, K., Badet, B., Walsh, C.T., Tanaka, H. and Soda, K. (1986). Thermostable alanine racemase from *Bacillus strearothermophilus*: Molecular cloning of the gene, enzyme purification and characterization. *Biochemistry, 25*: 3268 –3274.

Isom, D.G., Castaneda, CA., Cannon, B.R., Velu, P.D and Garcia-Moreno, E.B (2010). Charges in the hydrophobic interior of proteins. *Proceedings of the National Academy of Sciences of the United States of America, 107*: 16096 –16100.

Iyer, P.V. and Ananthanarayanan, L. (2008). Enzyme stability and stabilization − aqueous and non-aqueous environment. *Process Biochemistry, 43*: 1019 –1032.

Jana, S., Chaudhuri, T.K. and Deb, J.K. (2006). Effects of guanidine hydrochloride on the conformation and activity of *steptomycin adenylyltransferase* monitored by circular dichroism and fluorescence spectroscopy. *Biochemistry, 71*: 1230 – 1237.

Jeang, C.L., Chen, L.S., Chen, M.Y., Shiau, R.J. (2002). Cloning of a gene encoding raw-starch digesting amylase from a *Cytophaga* sp. And its expression in *Escherichia coli*. *Applied and Environmental Microbiology, 68*: 3651 –3654.

Joel, E.L. and Bhima, B.V. (2012). Production of alpha amylase by mangrove associated fungi *Pestalotiopsis microspora* strain VB5 and *Aspergillus oryzae* strain VB6. *Indian Journal of Geo-Marine Sciences, 41*: 279 –283.

Kadziola, A., Abe, J., Svensson, B. and Haser, R. (1994). Crystal structure of barley α-amylase. *Journal of Molecular Biology*, *239*: 104 –121.

Khajeh, K., Ranjbar, B., Naderi-Manesh, H., Habibi, A.E. and Gorgani, M.N. (2001). Chemical modification of bacterial α-amylases: Changes in tertiary structures and the effect of additional calcium. *Biochimica et Biophysica Acta*, *1548*: 229 – 237.

Kim, J., Nanmori, T. and Shinke, R. (1989). Thermostable, raw-starch-digesting amylase from *Bacillus stearothermophilus*. *Applied and Environmental Microbiology, 55*: 1638–1639.

Krishnan, T. and Chandran, A.K. (1983). Purification and characterization of α-amylase from *Bacillus licheniformis* CUMC305. *Applied and Environmental Microbiology, 46*: 430 –437.

Kruger, J.E. and Lineback D.R. (1987). Charbohydrate degrading enzymes in cereals. In J.E. Kruger, D.R. Lineback and C.E. Stautter (Eds.), *Enzyme and Their Role in the Cereal Technology* (pp. 117-139). Minnesota AACC.

Kumari, A., Rosenkranz, T., Kayastha, A.M. and Fitter, J. (2010). The effect of calcium

binding on the unfolding barrier: A kinetic study on homologous α-amylases. *Biophysical Chemistry, 151*: 54 –60.

Kunamneni, A., Permaul, K. and Singh, S. (2005). Amylase production in solid state fermentation by the thermophilic fungus *Thermomyces lanuginosus*. *Journal of Biosciences and Bioengineering, 100*: 168 –171.

Lai, Z., McCulloch, J., Lashuel, H.A. and Kelly, J.W. (1997). Guanidine hydrochloride-induced denaturation and refolding of transthyretin exhibits a marked hysteresis: Equilibria with high kinetic barriers. *Biochemistry*, *36*: 10230 –10239.

Lefuji, H., Chino, M., Kato, M. and Limura, Y. (1996). Raw starch-digesting and thermostable α-amylase from the yeast *Cryptococcus* sp. S-2: Purification, characterization, cloning and sequencing. *Biochemical Journal, 318*: 989 –996.

Lin, L., Chyau, C. and Hsu, W.H. (1998). Production and properties of a raw starch-degrading amylase from thermophilic and alkaliphilic *Bacillus* sp. TS-23. *Biotechnology and Applied Biochemistry, 28*: 61 –68.

Liu, X.D. and Xu, Y. (2008). A novel raw starch digesting α-amylase from a newly isolated *Bacillus* sp. YX-1: Purification and characterization. *Bioresource Technology*, *99*: 4315 –4320.

Liu, Y., Lu, F., Li, Y., Wang, J. and Gao, C. (2008). Acid stabilization of *Bacillus licheniformis* alpha amylase through introduction of mutations. *Applied Microbiology and Biotechnology, 80*: 795 –803.

Luke, K.A., Higgins, C.L. and Wittung-stasfshede, P. (2007). Thermodynamic stability and folding of proteins from hyperthermophilic organisms. *FEBS Journal, 274*:

4023 –4033.

Machius, M., Declerck, N., Huber, R. and Wiegand, G. (1998) Activation of *Bacillus licheniformis* α-amylase through a disorder to order transition of the substrate-binding site mediated by a calcium-sodium-calcium metal triad. *Structure*, *6*: 281–292.

Machius, M., Declerck, N., Huber, R. and Wiegand, G. (2003). Kinetic stabilization of *Bacillus licheniformis* alpha-amylase through introduction of hydrophobic residues at the surface. *Journal of Biological Chemistry*, *278*: 11546 –11553.

Machius, M., Wiegand, G. and Huber, R. (1995). Crystal structure of calcium-depleted *Bacillus licheniformis* α-amylase at 2.2 Å resolution. *Journal of Molecular Biology, 246*: 545 –559.

Matsubara, T., Ben Ammar, Y., Anindyawati, T., Yamamoto, S., Ito, K., Lizuka, M. and Minamiura, N. (2004). Degradation of raw starch granules by α-amylase purified from culture of *Aspergillus awamori* KT-11. *Journal of Biochemistry and Molecular Biology, 37*: 422–428.

McTigue, M.A., Kelly, C.T., Doyle, E.M. and Fogarty, W.M. (1995). The alkaline amylase of the alkalophilic *Bacillus* sp. IMD 370. *Enzyme and Microbial Technology, 17*: 570 –573.

Miller S., Jannin, J., Lesk, A.M. and Chltonia, C. (1987). Interior and surface of monomeric proteins. *Journal of Molecular Biology*, *196*: 641 –656.

Motono, C., Oshima, T. and Yamagishi, A. (2001). High thermal stability of 3-isopropylmalate dehydrogenase from *Thermus thermophilus* resulting from low

DeltaC(p) of unfolding. *Protein Engineering*, *14*: 961–966.

Muzammil, S., Kumar, Y. and Tayyab, S. (2000) Anion-induced stabilization of human serum albumin prevents the formation of intermediate during urea denaturation. *Proteins: Structure, Function and Genetics, 40*: 29 –38.

Nagarajan, D.R., Rajagopalan, G. and Krishnan, C. (2006). Purification and characterization of a maltooligosaccharide-forming α-amylases from a new *Bacillus subtilitis* KCC 103. *Applied Microbiology and Biotechnology*, *73*: 591–597.

Najafi, M.F. and Deobagkar, D. (2005). Purification and characterization of an extracellular α-amylase from *Bacillus subtilitis* AX20. *Protein Expression and Purification, 41*: 349 –354.

Nakajima, R., Imanaka, T. and Aiba, S. (1985). Nucleotide sequence of the *Bacillus stearothermophilus* alpha-amylase gene. *Journal of Bacteriology, 163*: 401–406.

Nazmi, A.R., Reinisch, T. and Hinz, H.J. (2006). Ca-binding to *Bacillus licheniformis* α-amylase (BLA). *Archives of Biochemistry and Biophysics*, *453*: 18 –25.

Nazmi, A.R., Reinisch, T. and Hinz, H.J. (2007). Calorimetric studies on renaturation by CaCl$_2$ addition of metal-free α-amylase from *Bacillus licheniformis* (BLA). *Journal of Thermal Analysis and Calorimetry*, *91*: 141–149.

Nielsen, J.E. and Brochert, T.V. (2000). Protein engineering of bacterial α-amylases. *Biochimica et Biophysics. Acta*, *1543*: 253 –274.

Nozaki, Y. (1972) The preparation of guanidine hydrochloride. *Methods in Enzymology*,

26: 43–50.

Offen, W.A., Viksoe-Nielsen, A., Borchert, T.V., Wilson, K.S. and Davies, G. J. (2015). Three-dimensional structure of a variant 'Termamyl-like' *Geobacillus stearothermophilus* α-amylase at 1.9Å resolution. *Acta Crystallographica Section F: Structural Biology Communications*, *71*: 66 –70.

Okolo, B.N., Ire, F.S., Ezeogu, L.I., Anyanwu, C.U. and Odibo, F.J.C. (2000). Purification and some properties of a novel raw starch-digesting amylase. *Journal of the Science of Food and Agriculture, 81*: 329 –336.

Oliveira, M.C., Teixeira, R.D., Andrade, M.O., Pinheiro, G.M., Ramos, C.H.I. and Farah, C.S. (2015). Cooperative substrate binding by a diguanylate cyclase. *Journal of Molecular Biology, 427*: 415 –432.

Omemu A.M., Akpan, I., Bankole, M.O. and Teniola, O.D. (2005). Hydrolysis of raw tuber starches by amylase of *Aspergillus niger* AM07 isolated from the soil. *African Journal of Biotechnology, 4*: 19 –25.

Pace, C.N., Alston, R.W. and Shaw, K.L. (2000). Charge-charge interactions influence the denatured state ensemble and contribute to protein stability. *Protein Science*, *9*: 1395–1398.

Pace, C.N., Grimsley, G.R. and Sholtz, J.M. (2009). Protein ionizable groups: pK values and their contribution to protein stability and solubility. *Journal of Biological Chemistry, 284*: 13285 –13289.

Pace, C.N., Shirley, B.A. and Thomson, J.A. (1989). In T.E. Creighton, (Ed.), *Protein Structure: A Practical Approach* (pp. 311–330). New York: Oxford University

Press.

Pandey, A., Nigam, P., Soccol, C.R., Soccol, V.T., Singh, D. and Mohan, R. (2000). Advances in microbial amylases. *Biotechnology and Applied Biochemistry, 31*: 135 –152.

Paquet, V., Croux, C., Goma, G. and Soucaille, P. (1991). Purification and characterization of the extracellular α-amylase from *Clostridium acetobutylicum* ATCC 824. *Applied and Environmental Microbiology, 57*: 212 –218.

Park, J-T., Suwanto, A., Tan, I., Nuryanto, T., Lukman, R. and Jane, J-L. (2014). Molecular cloning and characterization of a thermostable α-amylase exhibiting an unusually high activity. *Food Science and Biotechnology*, *23*: 125 –132.

Primarini, D. and Ohta, Y. (2000). Some enzyme properties of raw starch digesting amylases from *Streptomyces* sp. no. 4. *Starch-Starke, 52*: 28 –32.

Ptitsyn, O.B., Pain, R.H., Semisotnov, G.V., Zerovnik, E. and Razgulyaev, O.I. (1990). Evidence for a molten globule state as a general intermediate in protein folding. *FEBS Letters*, *262*: 20 –24.

Ramos, C.H.I. and Baldwin, R.L. (2002). Sulfate anion stabilization of native ribonuclease A both by anion binding and by the Hofmeister effect. *Protein Science, 11*: 1771 –1778.

Rashid, F., Sharma, S. and Bano, B. (2005). Comparison of guanidine hydrochloride (GdnHCl) and urea denaturation on inactivation and unfolding of human placental cystatin (HPC). *The Protein Journal, 24*: 283 –292.

Rizzolo, L.J. and Tanford, C. (1978). Denaturation of the tryptic fragments of the calcium (II) adenosine triphosphatase from sarcoplasmic reticulum by guanidinium hydrochloride. *Biochemistry, 17*: 4044 –4048.

Roseman, M. and Jencks, W.P. (1975). Interaction of urea and other polar compounds in water. *Journal of the American Chemical Society*, *97*: 631-640.

Roy, J.K. and Mukherjee, A.K. (2013). Applications of a high maltose forming, thermo-stable α-amylase from an extremely alkalophilic *Bacillus licheniformis* strain AS08E in food and laundry detergent industries. *Biochemical Engineering Journal, 77*: 220-230.

Saito, N. (1973). A thermophilic extracellular α-amylase from *Bacillus licheniformis.* *Archives of Biochemistry and Biophysics, 155*: 290 –298.

Sancho, J. (2013). The stability of 2-state, 3-state and more-state proteins from simple spectroscopic techniques... plus the structure of the equilibrium intermediates at the same time. *Archives of Biochemistry and Biophysics, 531*: 4 –13.

Satoh, E., Uchimura, T., Kudo, T. and Komagata, K. (1997). Purification, characterization and nucleotide sequence of an intracellular maltotriose-producing α-amylase from *Streptococcus bovis* 148. *Applied and Environmental Microbiology, 63*: 4941–4944.

Selkoe, D.J. (2004). Cell biology of protein misfolding: The examples of Alzheimer's and Parkinsons's diseases. *Nature Cell Biology, 6:* 1054 –1061.

Shaw, B.F., Schneider, G.F., Bilgicer, B., Kaufman, G.K., Nevenu, J.M., Lane, W.S., Whitelegge, J.P. and Whitesides, G.M. (2008). Lysine acetylation can generate

highly charged emzymes with increased resistance towards irreversible inactivation. *Protein Science, 17*: 1446 –1455.

Shiraki, K., Nishikori, S., Fujiwara, S., Hashimoto, H., Kai, Y., Takagi, M. and Imanaka, T. (2004). Comparison of the molten globule states of thermophilic and mesophilic α-amylases. *Biophysical Chemistry*, *122*: 58 –65.

Shokri, M.M., Khajeh, K., Alikhajeh, J., Asoodeh, A., Ranjbar, B., Hosseinkhani, S. and Sadeghi, M. (2006). Comparison of the molten globule states of thermophilic and mesophilic α-amylases. *Biophysical Chemistry, 122*: 58 –65.

Singh, K. and Kayastha, A.M. (2014). α-Amylases from wheat (*Triticum aestivum*) seeds: Its purification, biochemical attributes and active site studies. *Food Chemistry, 162*: 1 –9.

Sogami, M. and Ogura, S. (1973). Structural transitions of bovine plasma albumin: Location of tyrosyl and tryptophyl residues by solvent perturbation difference spectra. *Journal of Biochemistry, 73*: 323 –334.

Souza D.P.M. and Magalhaes O.D.P. (2010). Application of microbial α-amylase in industry – A review. *Brazillian Journal of Microbiology, 41*: 850 –861.

Sterner, R. and Liebl, W. (2001). Thermophilic adaptation of proteins. *Critical Reviews in Biochemistry and Molecular Biology*, *36*: 39 –106.

Strucksberg, K.H., Rosenkranz, T. and Fitter, J. (2007). Reversible and irreversible unfolding of multi-domain proteins. *Biochimica et Biophysics Acta*, *1774*: 1591– 1603.

Sun, H., Ge, H. and Zhang, W. (2007). Production of a novel raw-strach degrading enzymes. *Applied Biochemistry and Biotechnology, 160:* 988 –1003.

Sundram, A. and Murthy, T.P.K. (2014). α-Amylase production and application: A review. *Journal of Applied and Environmental Microbiology, 24*: 166 –175.

Takkinen, K., Pettersson, R.F., Kalkkinen, N., Palva, I., Soderlund, H. and Kaariainen, L. (1983). Amino acid sequence of alpha-amylase from *Bacillus amyloliquefaciens* deduced from the nucleotide sequence of the cloned gene. *Journal of Biological Chemistry*, *258*, 1007 –1013.

Tan, C.Y., Rahman, R.N., Kadir, H.A. and Tayyab, S. (2011). Conformational destabilization of *Bacillus licheniformis* alpha-amylase induced by lysine modification and calcium depletion. *Acta Biochimica Polonica*, *58*: 405 –412.

Tan, C.Y., Rahman, R.N.Z., Kadir, H.A. and Tayyab, S. (2010). Calcium-induced stabilization of α-amylase against guanidine hydrochloride denaturation. *African Journal of Biotechnology*, *9*: 7934-7941.

Tanford, C. (1968). Protein denaturation. *Advances in Protein Chemistry, 23*: 121 –282.

Tanford, C. (1997). How protein chemists learned about the hydrophobic factor. *Protein Science*, *6*: 1358 – 1366.

Tayyab, S. and Qasim, M.A. (1986). A correlation between changes in conformation and molecular properties of bovine serum albumin upon succinylation. The *Journal of Biochemistry, 100*: 1125 –1136.

Tayyab, S., Qamar, S. and Islam, M. (1991). Size exclusion chromatography and size

exclusion HPLC of proteins. *Biochemical Education, 19*: 149 –152.

Tomazic, S.J. and Klibanov, A.M. (1988). Why is one *Bacillus* α-amylases more resistant against irreversible thermoinactivation than another? *Journal of Biological Chemistry*, *263*: 3092 – 3096.

Tsytlonok, M. and Itzhaki, L.S. (2013). The how's and why's of protein folding intermediates. *Archives of Biochemistry and Biophysics, 531*: 14 –23.

Ugwu, S.O. and Apte, S.P. (2004). The effect of buffers on protein conformational stability. *Journal of Pharmacology and Technology, 28*: 86 –113.

Ulrika, B.E., Hallberg, B.M., Detitta, G.T., Dekker, N. and Nordlund, P. (2006). Thermofluor-based high-throughput stability optimization of proteins for structural studies. *Analysis Biochemistry*, *357*: 289 – 298.

Vielle, C. and Zeikus, G.J. (2001). Hyperthermophilic enzymes: Sources, uses and molecular mechanisms for the thermostability. *Microbiology and Molecular Biology Reviews, 65*: 1–43.

Vihinen, M. and Matsala, P (1989). Microbial amylolytic enzymes. *Critical Reviews in Biochemistry and Molecular Biology, 24*(4): 329 – 418.

Violet, M. and Meunier, J.C. (1989). Kinetic studies of the irreversible thermal inactivation of *Bacillus licheniformis* α-amylase. *Biochemical Journal, 26*: 665 – 670.

Wood, S.J., Maleef, B., Hart, T. and Wetzel, R. (1996). Physical, morphological and functional differences between pH 5.8 and 7.4 aggregates of the Alzheimer's

amyloid peptide A β. *Journal of Molecular Biology*, *256*: 870 –877.

Wu, X., Ge, J., Yang, C., Hou, M. and Liu, Z. (2015). Facile synthesis of multiple enzyme-containing metal-organic frameworks in a biomolecule-friendly environment. *Chemical Communications*, *51*: 13408-13411.

Yuuki, T., Nomura, T., Tezuka, H., Tsuboi, A., Yamagata, H., Tsukagoshi, N. and Udaka S. (1985). Complete nucleotide sequence of a gene coding for heat- and pH-stable α-amylase of *Bacillus licheniformis*: Comparison of the amino acid sequences of three bacterial liquefying α-amylases deduced from the DNA sequences. *Journal of Biochemistry, 98*: 1147-1156.

Zhang, C., Gao, C., Mu, J., Qiu, Z. and Li, L. (2013). Spectroscopic studies on unfolding processes of apo-neuroglobin induced by guanidine hydrochloride and urea. *BioMed Research International, 2013*: 7

Zhang, H., Kaneko, K., Nguyen, J.T., Livshits, T.L., Baldwin, M.A., Cohen, F.E., James, T.L. and Prusiner, S.B. (1995). Conformational transitions in peptides containing two putative α-helicals of the the prion protein. *Journal of Molecular Biology, 250:* 514 –526.

LIST OF PUBLICATION AND PRESENTATION

1. **Kandandapani, S.,** Tan, C.Y., Shuib, A.S. and Tayyab, S. (2016). Influence of buffer composition and calcium chloride on GdnHCl denaturation of *Bacillus licheniformis* α- amylase. *Protein & Peptide Letters*, *23*(6): 537 –543.

2**.** **Kandandapani, S.,** Wong, Y.H., Shuib, A.S. and Tayyab, S. (2015). Guanidine hydrochloride-denatured states of *Bacillus licheniformis* α-amylase under different buffer conditions. Proceedings of the 40th Annual Conference of the Malaysian Society for Biochemistry & Molecular Biology held at Putrajaya Marriot Hotel, on June 10-11 June 2015. Abstract No.16, pp 56.

BIOGRAPHY

Salanee Kandandapani was born in Selangor, Malaysia on 20th February 1988. She joined Asia Metropolitan University College in 2006–2009 and obtained her diploma in Pharmacy. She continued her studies in 2010 as an undergraduate student of Biomedical Sciences and obtained her B.Sc. degree in 2013. During 2014–2015, she served as a Research Assistant in the UMRG Project (RG275/14AFR) at the Institute of Biological Sciences, Faculty of Science, University of Malaya. She registered as a postgraduate student in Biochemistry (by research) at the University Malaya in 2015. She has been the recipient of the University Malaya Fellowship for the period 2015-2016 during her masters programme.

Influence of Buffer Composition and Calcium Chloride on GdnHCl Denaturation of *Bacillus licheniformis* α-Amylase

Salanee Kandandapani, Cheau Y. Tan, Adawiyah S. Shuib and Saad Tayyab*

Biomolecular Research Group, Biochemistry Programme, Institute of Biological Sciences, Faculty of Science, University of Malaya, 50603 Kuala Lumpur, Malaysia

Saad Tayyab

Abstract: The influence of buffer composition on the conformational stability of native and calcium-depleted *Bacillus licheniformis* α-amylase (BLA) was investigated against guanidine hydrochloride (GdnHCl) denaturation using circular dichroism, fluorescence and UV-difference spectroscopy. Differential effect of buffer composition on GdnHCl denaturation of BLA was evident from the magnitude of these spectral signals, which followed the order: sodium phosphate > Tris-HCl > HEPES > MOPS. These effects became more pronounced with calcium-depleted BLA. Sephacryl S-200 gel chromatographic results showed significant BLA aggregation in the presence of 6 M GdnHCl.

Keywords: α-Amylase, *Bacillus licheniformis*, Calcium, Denaturation, Fluorescence spectroscopy, Guanidine hydrochloride.

1. INTRODUCTION

Proteins preserve their native globular structures in order to displaying their biological functions. This conformational state of a protein, unique to itself, is formed as a result of folding involving different non-covalent interactions and disulfide bonds. Under specific conditions *i.e.* pH, temperature, pressure and salinity, a protein has to maintain its native globular structure to prevent loss of biological activity [1-3]. An enzyme's biological activity in solution is build upon its three-dimensional conformation, which in turn is governed by its amino acid sequence [4]. While many enzymes are obtained from psychrophiles and mesophiles [5,6], thermophilic or hyperthermophilic organisms offer greater advantage as a source of enzymes for industrial use, which in most cases involve endothermic processes [7,8].

α-Amylases (α-1,4-glucan-4-glucanohydrolases, EC 3.2.1.1), members of the endo-amylase family, catalyze the cleavage of α-D-(1,4) glycosidic linkages of starch [9]. These enzymes are long established in industries involving starch processing, beverage, textile and detergent technologies [10]. In view of the industrial operations at high temperatures, thermostable α-amylases specifically from the *Bacillus* genus have attracted greater attention in modern industrial practices [11-14]. *Bacillus licheniformis* α-amylase (BLA) has shown remarkable thermostability with a T_m value of 103°C [15,16]. BLA consists of a single polypeptide chain of 483 amino acid residues, arranged in three domains [17]. The enzyme possesses three calcium binding sites, two of which are located in domain B, while the third one is present at the interface between domains A and C [18]. Calcium

ions are known to play important role in BLA stability [19-22]. In earlier reports, we have shown calcium-induced stabilization of BLA against GdnHCl denaturation [23,24].

Aqueous, ready-to-use enzyme solutions are preferred for industrial applications. However, most of these are not stable in solution for a long period. Hence, additives in enzyme formulation such as metal ions [25,26] and other stabilizing agents including buffer components are used to stabilize the enzyme [27]. Buffers, such as cacodylate, MES, HEPES, Tris and phosphate buffers have been found to produce differential effects with respect to deoxynucleotidyl transferase-catalyzed polymerization of deoxynucleoside triphosphates [28]. This prompted us to investigate the effect of buffer composition on BLA stability against GdnHCl. Here, we present our data on GdnHCl denaturation of BLA in the presence of different buffers (sodium phosphate, Tris-HCl, HEPES, MOPS) using commercial BLA as well as calcium-depleted BLA preparations, employing far-UV circular dichroism, intrinsic fluorescence and UV difference spectroscopy.

2. MATERIALS AND METHODS

2.1. Materials

α-Amylase from *Bacillus licheniformis* (BLA) (Lot No. 018K7008), guanidine hydrochloride (GdnHCl) (≥ 99 % pure), ethylene glycol-bis(2-aminoethylether)-N,N, N',N'-tetraacetic acid (EGTA), MOPS, sodium salt, HEPES, sodium salt, sodium dihydrogen phosphate and di-sodium hydrogen phosphate were purchased from Sigma-Aldrich Inc., USA. Tris base was obtained from AMRESCO®, USA while calcium chloride (CaCl₂) was the product of SYSTERM®, Malaysia. The commercial BLA preparation (partially saturated with calcium) was used as such in these studies without any further treatment and is termed as BLA / native BLA.

*Address correspondence to this author at the Biomolecular Research Group, Biochemistry Programme, Institute of Biological Sciences, Faculty of Science, University of Malaya, 50603 Kuala Lumpur, Malaysia;
Tel: +603 7967 7118; Fax: +603 7967 4178;
E-mail: saadtayyab2004@yahoo.com